CHALMERS

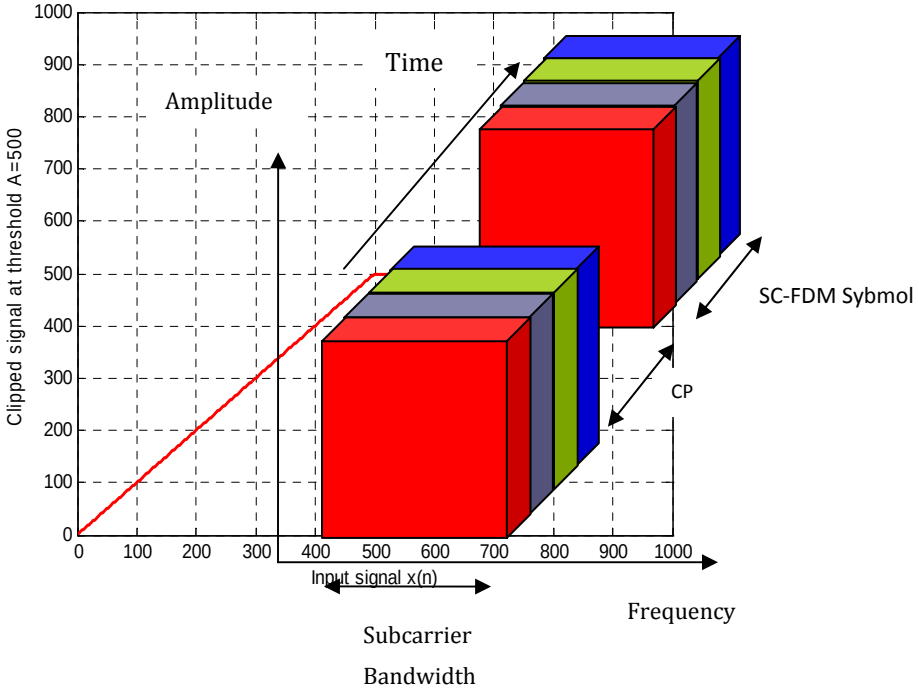

Uplink Power Control for IMT-Advanced

Master's Thesis in the Master Degree Programme, Communication Engineering

Mujeeb Ur Rehman

Fahad Muslim

Department of Signals and Systems

CHALMERS UNIVERSITY OF TECHNOLOGY
Göteborg, Sweden, 2010 Ex018/2010
Authors contributed equally to this work.

Uplink Power Control for IMT-Advanced

Thesis for the degree of Master of Science

Cover page: The first figure represent a threshold clipping device used to model the non-linear amplifier while the second one shows the SC-FDMA scheme used in the uplink to lower the PAPR ratio that increases the amplifier efficiency.

ABSTRACT

The challenges in the wireless world are basically creating motivations to bring advanced techniques to improve not only the data rates but also the quality of service for users in mobile communication. Development is an ongoing process that has enhanced the different chain of standards like Global Systems for Mobile communications (GSM), Universal Mobile Telecommunications System (UMTS), Code Division Multiple Access (CDMA) and Long Term Evolution (LTE) and now International Mobile Telecommunication (IMT) Advanced is of our interest after LTE that has made a promise to give more services, capabilities, and better performance to the end users than any other radio interface technology has been able to give till date.

This thesis study involves the implementation of an IMT-Advanced uplink model for the bit error rate (BER) performance analysis of Turbo coding, different subcarrier mapping schemes e.g. Localized Frequency Division Multiple Access (LFDMA), Interleaved FDMA (IFDMA), Block Interleaved FDMA (BIFDMA) and Discrete Fourier Transform (DFT) pre-coding. These techniques have been implemented in linear and non-linear environments. Since pulse shaping has not been used so IFDMA performance analysis in non-linear environment was not possible with the non-linearity model used in this thesis. Hence the BER performance analysis in non-linear environments has been limited to BIFDMA and LFDMA schemes only. Non-linearities have been introduced by using a threshold clipping model using three different clipping percentages i.e. 1%, 10% and 30%. Moreover simulations have been performed for single user and multiuser environments, where we also analyzed the near far effect.

It has been found as expected that Turbo code performs better in the Additive White Gaussian Noise (AWGN) channel than in the Rayleigh-fading channel. DFT precoding is mainly intended to keep the Peak to Average Power Ratio (PAPR) value small, which is necessary for efficient performance of High Power Amplifiers (HPA), but it also gives slightly improved BER performance as compared to the non DFT precoded system. The single user BER performance for all the three mapping schemes is identical to the long term average BER performance of multiple users in linear environments. The performance in non-linear environments is however distorted in single user case mainly by Inter-carrier Interference (ICI) and in multiuser case by multi-access interference (MAI).

ACKNOWLEDGEMENTS

First of all we would like to thank Almighty ALLAH, the most merciful and beneficent, who always shows us the path of success and helps us in every moment of life and to whom we have to return one day.

Special thanks to our Examiner and Supervisor Ass. Prof Tommy Svensson, who is not only a good researcher but also a devoted supervisor who helped us at every stage and taught us the way the research, is done, you are really a nice person to work with. We are thankful to all those persons that helped us during our Masters Program. We are also grateful to Prof Erik Strӧm and Assoc. Professor Erik Agrell who not only supported us in different subjects but always provided a good guidance. We are also thankful to Johnny Karout, who always helped us and provided us guidance whenever we knocked his door.

Mujeeb: *"I am especially thankful to you Mother, your advices, wisdom, guidance and love have not only helped me at every step of life but also have given me a confidence to deal and solve every problem coming in my way and special thanks to my father who is not in this world but this was all his company and advices that I learned from. I am also thankful to my great sisters, brother in laws and my elder brother who is always there to guide me and help me. I am also thankful to all my friends in native country & in Sweden, room mates who were there to spread cheers around and help me, especially, Talha, Tabish and Umair. Finally I am thankful to Fahad for not only being a good thesis mate but also a cooperative and helping friend. I really enjoyed working with him. We together faced many difficult situations and were source of motivations for each other. I wish him good luck for his future life."*

Fahad: *"First of all, I would like to thank my parents for all they have done for me. It was only due to their prayers and their encouragement that made it possible for me to achieve whatever I have achieved up to now. I would also take this opportunity to thank my brother and my sisters whose support and affection has been very crucial for me. Very special thanks to my aunt who is one of my best friends and has done a lot for me and all my siblings. I always got words of encouragement whenever I talked to her. I would also like to thank all my friends here in Sweden. Without them my stay in Sweden would have been a very boring experience. They added flavor to my life here in Sweden. My special gratitude for my flat mates Afaq and Salman. My time spent with them has really been a memorable one. I would also like to thank Mujeeb. Working with him has been a nice experience. We both come from same country and that helped us to tune ourselves according to each other's style of work. Throughout our thesis work we have been through some very tough times where we apparently had no clue as to what is the right way out. It was his motivation towards the work that kept me motivated as well. I would like to wish him good luck in all his future endeavors."*

Contents

3. SIMULATIONS & RESULTS

4. CONCLUSIONS & FUTURE WORK

List of Figures

List of Acronyms

AWGN	Additive White Gaussian Noise
BER	Bit Error Rate
B-IFDMA	Block Interleaved Frequency Division Multiple Access
CCDF	Complementary Cumulative Distribution Function
CDMA	Code Division Multiple Access
CSIR	Channel State Information at the Receiver
DFT	Discrete Fourier Transform
EGPRS	Enhanced General Packet Radio Service
FDM/FDMA	Frequency Division Multiplexing/Multiple Access
FPLMTS	Future Public Land Mobile Telecommunications Systems
GPRS	General Packet Radio Service
GSM	Global Systems for Mobile Communications
HPA	High Power Amplifier
HSPA	High Speed Packet Access
ICI	Inter-carrier Interference
IFDMA	Interleaved Frequency Division Multiple Access
IMT	International Mobile Telecommunications
IP	Internet Protocol
ISI	Inter-symbol Interference
ITU-R	International Telecommunication Union Radio communication Sector
ISSL	Inband Subcarrier Set Leakage
LFDMA	Localized Frequency Division Multiple Access
LOS	Line Of Sight
LTE	Long Term Evolution
Mbps	Mega Bit Per Second
MMSE	Minimum Mean Square Error Equalizer
MAI	Multi Access Interference
OFDM	Orthogonal Frequency Division Multiplexing
OFDMA	Orthogonal Frequency Division Multiple Access
PAPR	Peak-To-Average Power Ratio
PDF	Probability Density Function
PS	Pulse Shaping
PCCC	Parallel concatenated convolutional code
SCCC	Serial concatenated convolutional codes
SC-FDE	Single Carrier with Frequency Domain Equalization
SC-FDMA	Single Carrier Frequency Division Multiple Access
TDMA	Time Division Multiple Access
TWT	Travelling wave tube
UMTS	Universal Mobile Telecommunications System
W-CDMA	Wideband Code Division Multiple Access
WINNER	Wireless World Initiative New Radio

CHAPTER 1

Introduction & Background

In this chapter the historical background regarding advancement in wireless communication has been described. It also includes the details about the objectives, scope and organization of the thesis.

1.1 Evolution of 3rd Generation Mobile Systems

It is said that "necessity is the mother of invention" and this was the reason that many rapid advancements were being made in the world of wireless communications over the years. Higher data rates and a better quality of service are always required by the users and this is what everything circulates around. The story begins with the invention of the 1st telephone by Alexander Graham Bell and since then, many rapid advancements took place till the 1st International mobile communications system Nordic Mobile Telephony (NMT) was introduced in 1981 at the same time when Advance Mobile Phone Service (AMPS) was introduced in North America. Due to some service issues in the First Generation System the Second Generation System (2G) emerged.

The second Generation Mobile System came with a good prospect of increasing the capacity and consistent quality of service using the digital communication system. The shift from analog to digital domain gave a great boost in the capacity, improved cost, speed and power efficiency of the digital hardware [1]. The primary services introduced in 2G were text SMS and circuit switched services enabling e-mail and other data applications. Multiple time slots were assigned to the users and coding schemes were modified. Later on 2.5G was introduced with some more latest services like GPRS and packet data over the cellular technologies [2].

Wireless communication is a field where rapid changes are taking place due to the need for high speed, high data rates and good quality of service which are the measures that bring advancements in the wireless world. This was the reason that 3G or UMTS emerged on the scene. The initial name for 3G was Future Public Land Mobile Telecommunications Systems (FPLMTS), which was later on changed to International Mobile Telecommunication (IMT-2000). ITU started the standardization process and defined the standard for 3G. The 3G system was intended to provide high speeds but also to provide a global mobility and various kinds of services including broadband and internet. As the time passed different types of improvements took place and the role of Third-Generation Partnership Project (3GPP) is very important to discuss here.

3GPP is a collaboration between groups of telecommunications associations that is developing the specifications for 3G Universal Terrestrial Radio Access (UTRA) and Global system for mobile communication (GSM). 3GPP is a partnership project formed by the different standard bodies [2]. 3GPP has published many releases among which in the

release 8 and 9 it has specified the specifications and enhancements of LTE. The latest release is the release 10.

1.2 Emergence of LTE

LTE is an abbreviation of "Long Term Evolution". This is an upgraded standard of UMTS. The standardization process of LTE was initiated in a workshop in November 2004. Different companies of broadband and mobile communications participated and presented their perceptions and requirements which needed to be satisfied. In the following, we have illustrated some of the major requirements and targets set for the LTE.

1.3 Requirements and Targets for the LTE

There are always some factors and needs for which a new technology arises and fills the gap left by the older technologies. The same is the case with LTE that comes with some objectives and targets. The requirements and targets were refined and finalized in June 2005. The key targets were like,

- Reducing the delays in terms of connection establishment and transmission
- Increasing the data rates and increasing the cell edge bit rate
- Reducing cost per bit in order to improve the spectral efficiency
- Creating a greater flexibility for spectrum usage, in both new and previously existing bands
- Creating simplified network architecture
- Seamless mobility, including mobility between different radio-access technologies
- Working on reasonable power consumption for the mobile terminals

The different releases of 3GPP have shown a tremendous development to achieve the requirements and targets for LTE.

1.4 LTE to IMT-Advanced

The 3GPP partners compiled a formal documentation and submitted it to ITU and proposed that LTE release 10 and beyond must be evaluated as a candidate for IMT-Advanced. The IMT-Advanced capabilities go beyond those of IMT 2000. The major features and characteristics of IMT-Advanced includes worldwide functionality, roaming, its compatibility of services with previous technologies, internetworking with other radio access systems, enhancing the data rates, services along with applications, also improving the deficiencies lying in the previous versions of LTE. In addition to the above features, one of the main reasons for aligning LTE with the call for IMT-Advanced is to make it a candidate for future new spectrum bands to be identified at WRC07.

If we take a look at the overall research areas and the community involved then there are many projects running in the area of IMT-Advanced and in the next generation of radio access. It will be worthwhile to discuss the WINNER project which was partly funded by the European Union [2]. The WINNER concept is very close to LTE, however it is concentrating more on the higher data rates and that's why it has been designed for a wider bandwidth than 20MHz. The WINNER is also working with the multi-hop modes and relaying concept. This is also true that the major stability and enhancements have been brought and settled by the standardization organizations [2].

So as a summary of the above discussion, we can say that the development is an ongoing process that always enhances the previous versions of technology and performance. The research is going on but the deployment and feedbacks from customers will make this process even faster. We have to admit that IMT-Advanced is still several years away whereas deployment of HSPA Evolution and LTE are in the process. High Speed Packet Access (HSPA) is a continuing evolution of the existing standards like WCDMA/HSPA technology whereas LTE is a new entrant and radio access optimized purely for IP based traffic. These two technologies have made a promise to give more services, capabilities, and performance to the end users than any other radio interface technology has been able to till date.

1. 5 Thesis Objectives

The basic objective of the thesis is to do some study, research and then writing out results in a presentable format through a report. In this part we have discussed briefly what we have done in different parts of the report.

1.5.1 SCOPE OF THE THESIS

In this thesis project firstly we observe the performance of different multiple access schemes on LTE Uplink. This requires the simulation of a time varying frequency selective channel and the simulated system should overcome the short comings of such channel like fading, Inter-Symbol Interference (ISI) and Inter-Carrier Interference (ICI). Then amplifier non-linearities are introduced by clipping the modulated signal to different amplitude clipping levels and analyzing its effect on the overall performance of the system. First of all a single user system is simulated followed by introducing more users and studying the effects on the overall system behavior. Finally the near far problem inherent in mobile cellular communications is considered in the system under study.

1.5.2 ORGANIZATION OF THE THESIS

In chapter 2 of this thesis report, readers are given an over view of the different building blocks present in the transceiver of the simulated system. Additionally all the blocks are explained briefly to give the readers an idea of what this thesis study was all about. The chapter covers different blocks in order as they occur in the system. The channel encoder is explained first, which is followed by modulation and the importance of pulse shaping. This is followed by a brief introduction of DFT precoding and different sub-carrier mapping schemes. OFDM modulation and amplifier non-linearities are introduced followed by some theory about power control. Finally we describe the fading channel and equalization to mitigate the adverse effects of wireless channels.

In chapter 3, readers are given details about the simulations and results obtained from those simulations. This includes presenting the various system parameters and describing what should the different system parameters be to keep the system safe from the wireless channel impairments i.e. ICI and ISI. Besides simulation parameters, the results deduced from the simulations are also being presented with discussions on those results.

In the final chapter of this thesis report we conclude our work and try to summarize what we have learnt from this thesis work and also we shed some light on what possible future work can be done in the areas covered in this master's thesis.

1.5.3 ASSESSMENT METHODOLOGY

The simulations have been performed in MATLAB. The channel model used is WINNER-C2 NLOS channel. It has been simulated using the spectrum method (see appendix A). First of all, all the blocks have been constructed individually and tested with an ideal channel to see if they are working properly. This is followed by introducing an AWGN channel and seeing if our BER curve resembles the theoretical BER curve. Finally the fading channel has been introduced and various results have been obtained thereafter by modifying the relevant system parameters for each aspect being tested. All the simulations have been carried out using the C3Se Linux Platform at Chalmers.

CHAPTER 2

SYSTEM MODEL

This Chapter includes the block by block description of the Shannon Model and the IMT-Advanced Uplink System Model. Before going to the simulations chapter, here the theoretical background is sketched related to channel coding, modulation, subcarrier mapping schemes, non-linear amplifier and power control.

2.1 Shannon Digital Communication Model

In a broader perspective a communication system consists of three main parts i.e. the transmitter, the receiver and the channel. In a digital communication system the information is transmitted in the form of binary digits or bits. The information source inputs bits into the transmitter, which processes the information and then it is transmitted over the channel. The channel distorts the signal through sources such as noise or interference and the role of the receiver is to retrieve the signal sent by the information source with certain precision.

Claude Shannon is rightly called the "Father of modern communications" as his communication model is the basis of modern communications. In this chapter we briefly describe the different blocks of Shannon's communication model which is shown in the figure below:

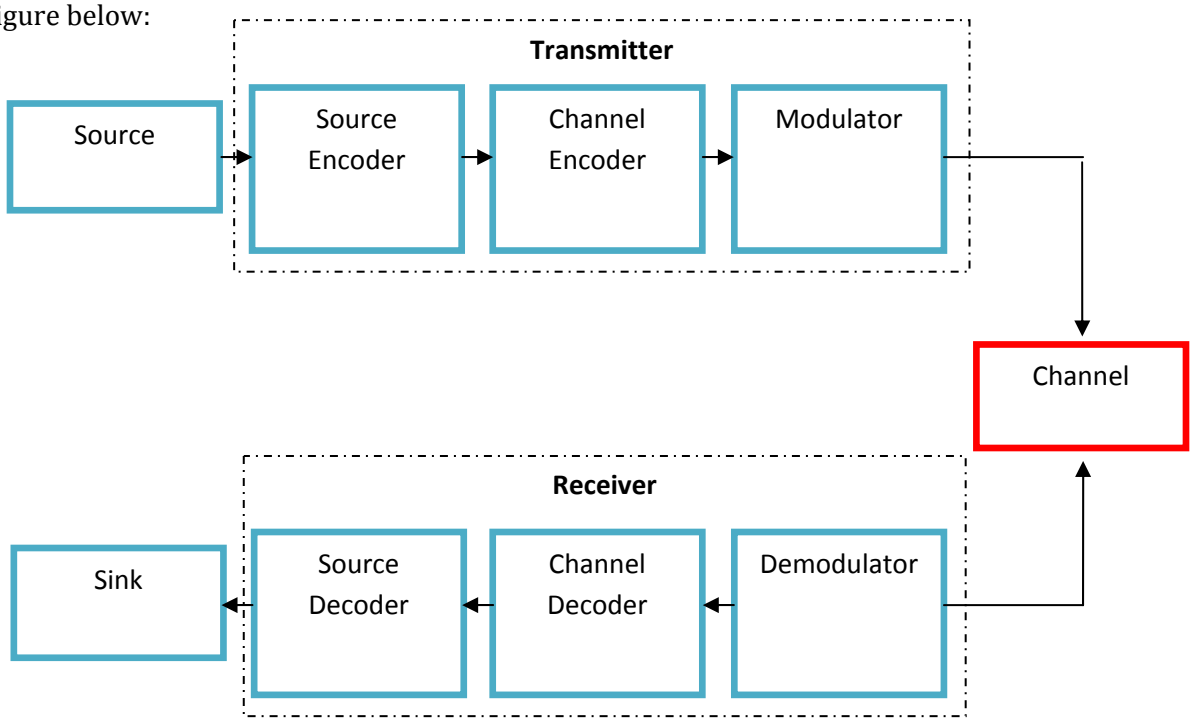

Figure 2.1: Shannon Communication Model

2.1.1 SOURCE ENCODER

Information theory says that any information can be represented in digital form by a number of bits depending on required fidelity. The source encoder here does this by representing the information from source into number of bits depending on end user's requirements [3].

2.1.2 CHANNEL ENCODER AND MODULATOR

Unlike the source encoder which removes redundancy, the channel encoder actually adds redundancy to the data to mitigate the channel distortions. The modulator then translates the encoded data into an analog waveform that can then be transmitted over the channel.

2.1.3 CHANNEL

The physical characteristics of the channel can vary widely and good channel models are necessary for designing efficient communication systems. The channel would corrupt the signal with distortions such as noise. The channel may be a wire line or wireless one and it has to be estimated somehow for efficient transmission across it.

2.1.4 DEMODULATOR AND CHANNEL DECODER

The demodulator then processes the received analog waveform which is actually a distorted version of the transmitted signal. The main tasks of the demodulator is to take care of synchronization between the clocks and oscillators at transmitter and receiver, and channel equalization to compensate for ISI introduced by a dispersive channel. Thus the demodulator's ultimate goal is to produce hard or soft decisions on the transmitted symbols to be fed into the channel decoder which then makes use of the redundancy in the coded data to improve upon the estimates from demodulator and to produce estimates of the sequence of information symbols that were input to the channel encoder [3].

2.1.5 SOURCE DECODER

The source decoder then converts the estimated information bits produced by the channel decoder into a form that can be used by the end user i.e. the sink [3].

2.2 IMT-Advanced Uplink Power Control System Model

In this section of the report we have discussed the different blocks of the IMT-Advanced Uplink System model, which we have developed and used it to analyse the BER performance of different sub-carrier mapping schemes (BIFDMA, IFDMA and LFDMA) and to see the impact of amplifier non-linearities.

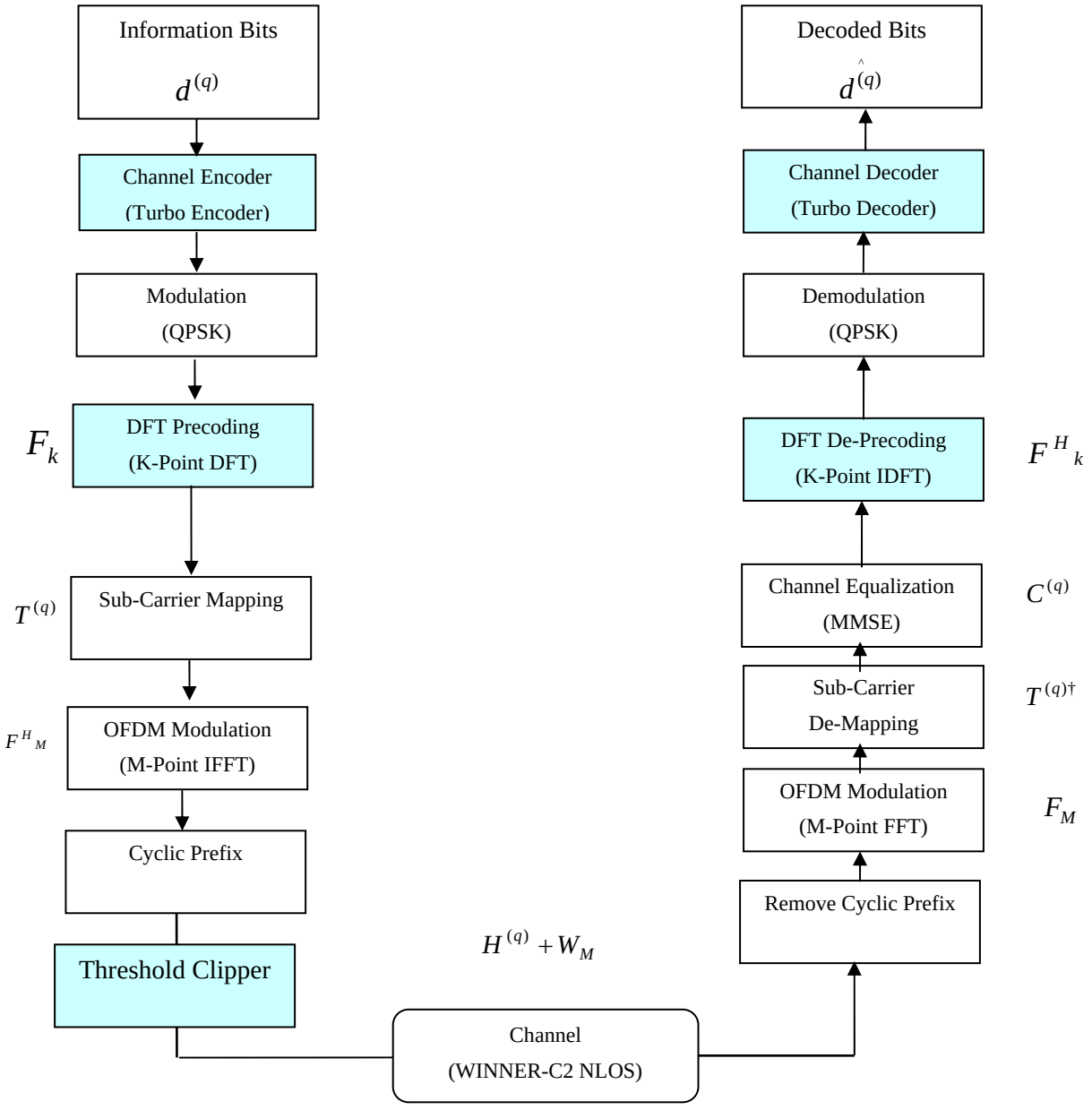

Figure 2.2: The IMT-Advanced model

We have used the IMT-Advanced model with different variations that are briefly described below,

1. Uncoded System

In this model we have used the same system without the Turbo coding blocks to see the performance of the system. Later on we have compared uncoded system results with coded system results.

2. Without DFT Precoded System

In this model we have removed the DFT precoding and DFT de-precoding blocks in order to see the effect of DFT precoding on the system under test.

3. Threshold clipping model

Threshold clipping model has been used to see the impact of amplifier non-linearities by using different clipping levels.

2.2.1 CHANNEL CODING

The basic objective of channel coding is to introduce redundant bits to save the information from channel impairments and to minimize the errors. There are different channel coding techniques used to mitigate the adverse effects of the wireless channels for example Block codes, Convolutional codes and Turbo codes. In this project we have used the Turbo code due to its efficient performance when dealing with large blocks of data.

Before going in to the details of Turbo codes here it is very necessary to mention about the history of Turbo codes. Turbo codes were developed by C. Berrou and A. Glavieux at the Ecole Nationale Superieure des Telecommunications de Bretagne in Brest, France, as an exercise in VLSI design [4]. The first proposed Turbo code was a parallel concatenated convolutional code (PCCC) with two convolutional codes with an interleaver between the two codes. The concatenated codes are basically divided into two types, one is parallel concatenated convolutional code (PCCC) and the other one is serial concatenated convolutional codes (SCCC) [4]. A very good performance from Turbo code can be achieved by passing larger blocks of data. In the following we have discussed about the structure and functionality of the Turbo encoder and decoder to understand the necessary background, applications and the performance of Turbo codes.

2.2.1.1 Turbo encoder

The Turbo encoder consists of two or more essential recursive systematic convolutional (RSC) encoders separated by a pseudo-random interleaver. It is not necessary that the encoders will be identical but normally they are identical. As an example a block diagram of a Turbo encoder is shown with systematic feedback convolutional encoders and an interleaver. The constraint-length is 3 with generator matrix G= [7, 5] *octal*.

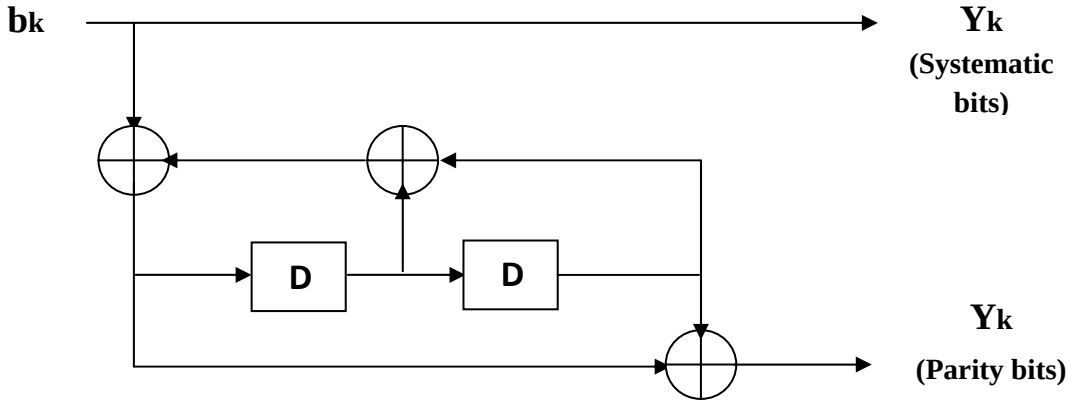

Figure 2.3: RSC encoder with generator matrix *G* = [7, 5] *octal*, constraint-length 3

In the figure the data bits "b_k" are generated and fed into the first encoder that generates a set of systematic and parity bits. The data bits are passed in to the second encoder after being altered by the pseudo-random interleaver. The second encoder also generates a similar set of bits while the over all code is punctured by deleting the second set of systematic bits. So the resulting bit stream consists of systematic bits from the first encoder followed by the parity bits from the first and second encoders, respectively. The overall code rate in this model is 1/3 while code rate can be varied to 1/2 by alternately puncturing the parity bits from each of the encoders before the transmission takes place.

By increasing the code rate, the bandwidth efficiency is increased while the performance of the system is ruined in terms of power efficiency [4]. Another essential and fundamental part of the Turbo code is the interleaver that is necessary to be described here with the encoder. There are different types of interleavers including block, pseudo-Random and convolutional Interleavers. The Turbo code performance is highly affected by the type of interleaver. With a few exceptions, random interleaver provides good performance [4].

2.2.1.2 Turbo decoder

A very effective feature of the Turbo code is the iterative decoding process. As an example in the following figure an iterative Turbo decoder has been shown that basically comprises of two soft input and soft output (SISO) decoding modules which are separated by an interleaver and a de-interleaver.

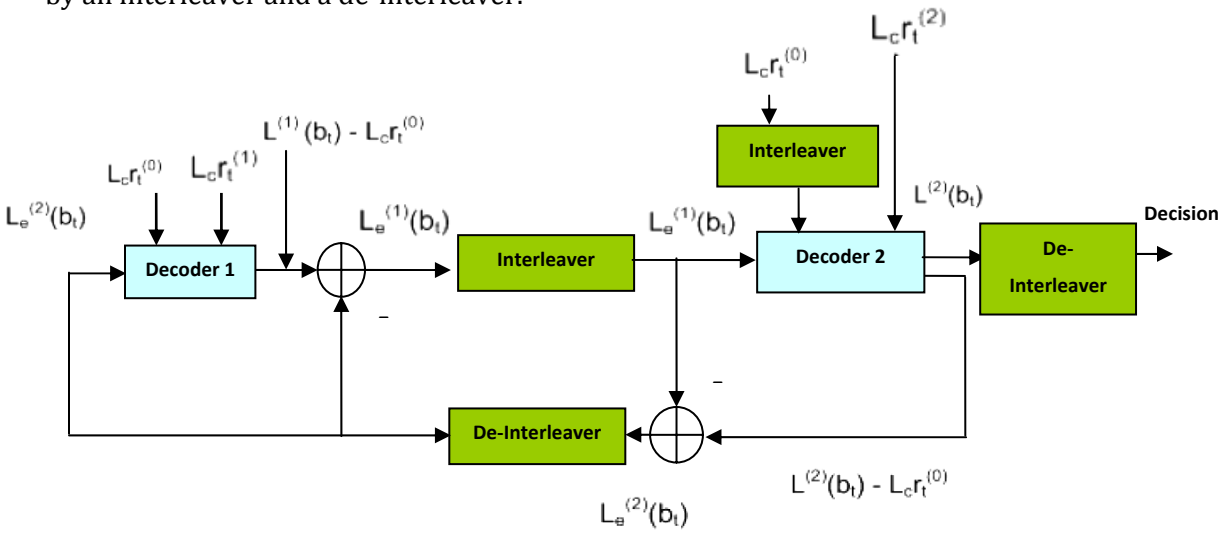

Figure 2.4: The Iterative Turbo decoder with two SISO decoding modules

The decoding process follows a decoding algorithm used by the SISO modules. There are two major types of trellis based algorithms that are used to decode the Turbo codes. One is the Viterbi algorithm and the other one is the Maximum A Posteriori (MAP) algorithm. The Viterbi algorithm accepts soft inputs and produces hard outputs while the MAP accepts soft inputs and produces soft outputs. The SISO algorithms are necessary for Turbo decoding as they share their extrinsic information with each other while they are computationally more complex. They also allow iterative sharing of results between decoders, which permits the use of powerful concatenated coding structures [4].

2.2.1.3 Performance of Turbo Codes

The Turbo codes are very efficient for processing long blocks of data but results in longer delays. There are some factors that affect the Turbo encoder performance. The major ones include the size of interleaver and the number of iterations on the decoder side. The figure 2.5 shows the performance of the Turbo code on the AWGN channel with different number of Iterations. As the number of Iterations is increased the performance gets better but the processing time is also increased [5].

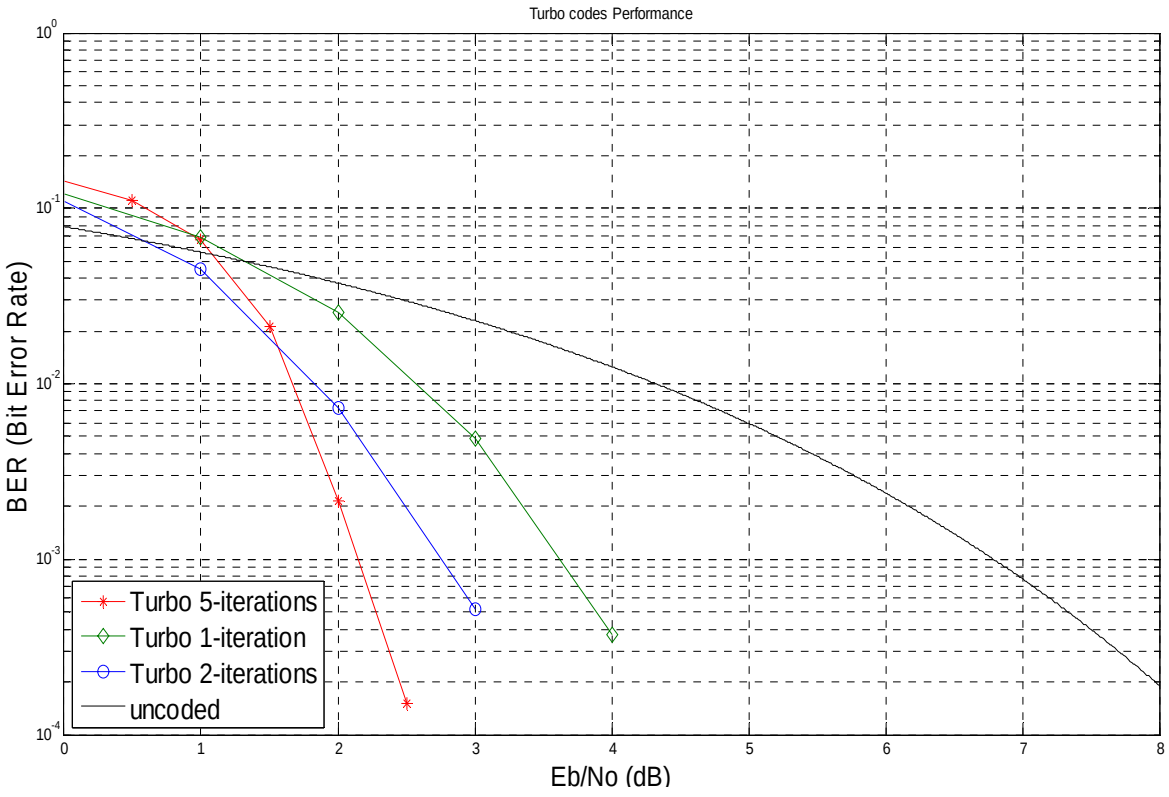

Figure 2.5: Turbo code BER Performance with Iterations (1, 2, and 5)

2.2.2 MODULATION AND PULSE SHAPING

In this section we will discuss about the base band modulation schemes (QPSK) and a brief description of pulse shaping will also be given.

2.2.2.1 Baseband modulation

Modulation is a technique in which one or more properties of a high frequency carrier signal is varied with respect to the modulating signal. The three main properties of carrier signals are its frequency, phase and its amplitude and hence the modulation can be frequency, phase and amplitude respectively depending on which property of the carrier is being varied. Quadrature amplitude modulation (QAM) is a technique in which the data is modulated both on the phase and amplitude of the carrier signal. Modulating digital data on an analog signal is called "Keying". So we have phase shift keying (PSK), frequency shift keying (FSK) and amplitude shifty keying (ASK) techniques to modulate digital data on the phase, frequency and amplitude of an analog signal respectively.

Here in this thesis the baseband modulation technique used is Quadrature Phase Shift Keying (QPSK) in which two bits are assigned to each symbol and which consists of four points in its constellation plot. The four constellation points are placed in each of the four quadrants of the signal space. They are equally spaced from the origin and can be seen as lying along the circumference of a circle with the origin representing the centre of the circle. Thus all the QPSK symbols have the same energy but have different phases. The axis lines thus become decision boundaries while each of the quadrants becomes the decision regions. The figure below shows a typical QPSK constellation plot consisting of four points along the circumference of a circle

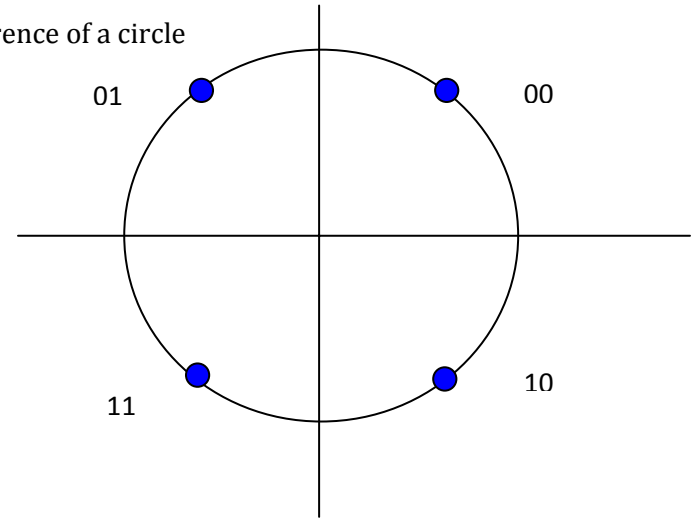

Figure 2.6: QPSK constellation diagram

It should be noted that the figure 2.6 depicts gray mapping in which each next symbol bit allocation differs from the neighbor symbols by a single bit. Since in QPSK we have two bits represented per symbol so a single symbol in error would correspond to two bits in error at the maximum. Grey mapping ensures that the most likely symbol errors would only cause a single bit in error. The theoretical bit error probability for QPSK modulation with the AWGN channel is given by

$$P_b = Q(\sqrt{\frac{2E_b}{N_o}}) \tag{2.1}$$

Where " E_b " is the average bit energy, " N_o " is the noise power spectral density and "Q" represents the Q-function.

2.2.2.2 Pulse shaping

With continuous advancements in communications and with the need of accommodating multiple users in a limited bandwidth, the bandwidth has become one scarce resource. Thus efforts are made to make an efficient use of this scarce resource. Pulse shaping filters are used to narrow bandwidth and to improve bandwidth usage. However, pulse shaping can introduce distortions and can increase the risk of inter symbol interference (ISI). These distortions make the design of an optimal receiver difficult [7]. The choice of pulse shaping filter is thus a tradeoff between bandwidth efficiency in frequency domain and ISI introduction in time domain. Hence pulse shaping filter is chosen to limit the bandwidth of the signal while minimizing the ISI in the system.

In order to better explain the concept of pulse shaping we would consider the most basic unit of digital transmission which is a simple rectangular pulse. Ideally the rectangular pulse has an infinite bandwidth but since in practical cases we have band limited channels hence the transmitted pulses tend to be "spread" during transmission. This pulse spreading would cause the pulses to overlap in adjacent time slots thus causing ISI [8].

One method of controlling ISI is to shape the transmitted pulses properly and one pulse shape that produces zero ISI is the sinc pulse which is shown in the figure below in time and frequency domain. The frequency response is just a rectangular waveform, band limited between -5 f_o and +5 f_o, where " f_o " is the pulse rate.

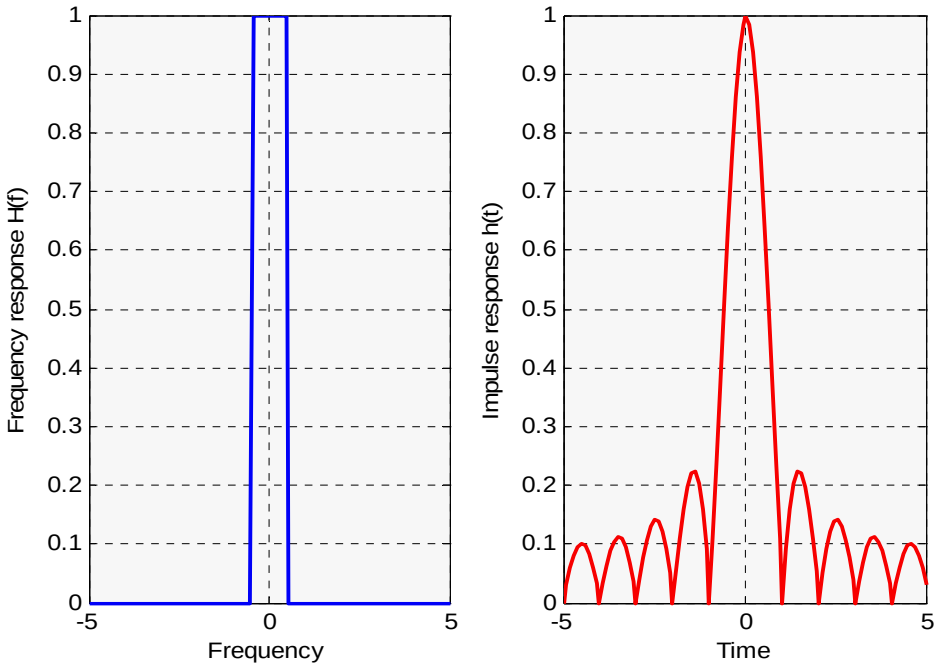

Figure 2.7: Frequency and impulse response of sinc pulse shaping filter

This filter shape is however practically unrealizable since an ideal low pass filter is not causal and also because this wave form critically depends on timing precision [8]. So for practical purposes an excess bandwidth factor "α" is used to spread the sinc pulse through some extra bandwidth which solves the problems with the sinc pulse. This new pulse is called the raised cosine pulse and the factor "α" is called roll off factor. The frequency response of this raised cosine filter is given in the equation below

$$HRC(f)=\begin{cases}\tau, |f| < \dfrac{1-\alpha}{2\tau} \\ \dfrac{\tau}{2}[1+\cos(\dfrac{\pi\tau}{2}(|f|)-(1-\alpha)/2\tau))], \dfrac{1-\alpha}{2\tau} \le |f| \le \dfrac{1+\alpha}{2\pi}| ; \\ 0; otherwise\end{cases} \tag{2.2}$$

Where "*f*" is the frequency and "τ" is the pulse interval. The impulse response is given as

$$h_{RC}(t)=\sin c(\frac{t}{T})\left[\frac{\cos(\frac{\pi\alpha t}{\tau})}{(1-(\frac{2\alpha t}{\tau})^2)}\right] \tag{2.3}$$

Where "*t*" is the time.

As the roll-off factor is increased from "0", at which the raised cosine pulse is nothing but a sinc pulse, the response characteristics of the raised cosine filter would change and we would move further and further away from the ideal rectangular shaped frequency response. The figures below show the impulse and frequency response of the raised cosine filter with different values of the roll-off factor.

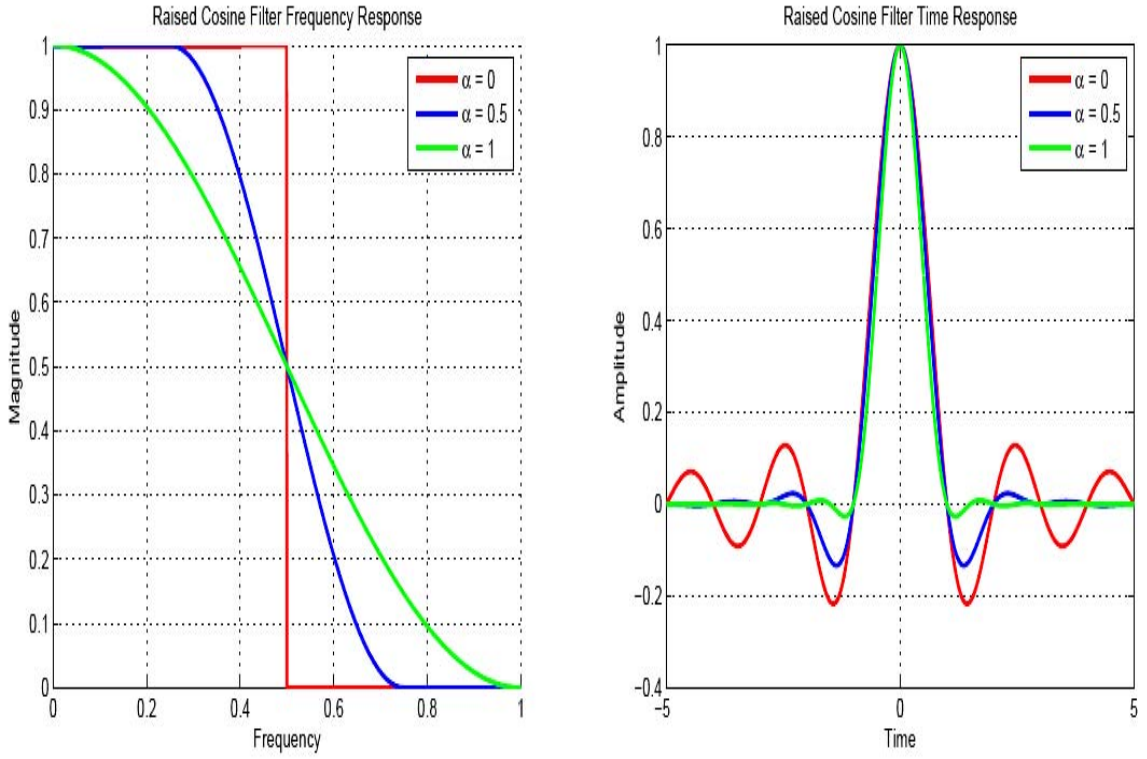

Figure 2.8: Frequency and Impulse response of RC filter at different values of α [9]

So we see that as the value of "α" increases from 0 to 1 the oscillations in the impulse response also increases while the impact in the frequency response can be seen in the form of more smooth transitions in the magnitude of frequency response as the value of "α" increases from 0 to 1. So the rectangular pulse after pulse shaping doesn't remain perfectly rectangular but is a smoothly rounded pulse consisting of ripples before and after the original period, and the amplitude of the ripples actually indicates what value of "α" is being used. So in short designing a pulse shaping filter requires a tradeoff between the bandwidth efficiency in frequency domain and ripple attenuation in the time domain. The tighter the bandwidth in frequency domain the higher the amplitude of side lobes would be in the time domain.

2.2.3 DFT PRECODING & DE-PRECODING

The DFT precoding & De-precoding blocks have been introduced in the uplink transmission in LTE and IMT-Advanced. The process of DFT precoding and De-precoding is very simple. In DFT precoding we take the K-point FFT of the modulated symbols while on the other side we need to take K-point IFFT of de-mapped symbols. This type of transmission scheme based on DFT precoded OFDMA is also called single carrier frequency division multiple access (SC-FDMA).

Some of the major advantages of SC-FDMA are to enable power efficient transmission in the uplink, improving the coverage, reducing the terminal cost and resulting in low envelop fluctuations of OFDMA signals [10]. DFT precoded OFDMA has much smaller peak to average power ratio (PAPR) than regular OFDM thus enabling very less complex and higher power terminals [11]. In this project we have seen the effect of DFT and Non- DFT precoding over the different carrier mapping schemes that will be discussed in the coming sections of the report.

2.2.4 SUBCARRIER MAPPING

The DFT precoded symbols coming out of the "DFT precoding" block are then mapped to a set of sub-carriers and the process is called sub-carrier mapping. The sub-carrier mapping block actually assigns the DFT complex values as amplitudes to some of the selected sub-carriers [12]. Usually a set of "N" sub-carriers is mapped to a set of "M" sub-carriers where M>N. Subcarrier mapping is of two main types: localized (LFDMA) and distributed (DFDMA) mapping. In localized mapping consecutive sub-carriers or a complete chunk (a time frequency unit in which the sub-carriers included essentially experiences flat fading) is assigned to users while in distributed mapping sub-carriers separated by some frequency offset are assigned to users.

Hence in localized mapping the sub-carriers are confined to some part of the total bandwidth while in distributed mapping the sub-carriers are assigned non-continuously over the whole bandwidth thus resulting in zero values for the remaining sub-carriers. A special case of the distributed mapping where the sub-carriers are separated equidistantly over the entire bandwidth is called interleaved SC-FDMA (IFDMA) [12]. It should be noted that DFT followed by the subcarrier mapping schemes effectively implements interpolation [13]. The figure below shows a generalized view of both the mapping schemes

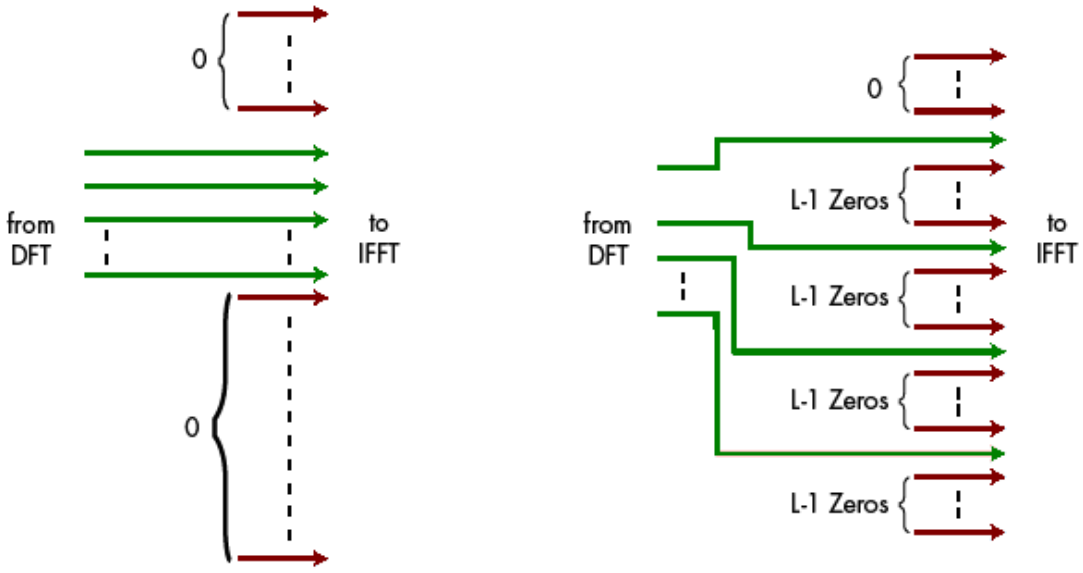

Figure 2.9: Localized mapping vs Distributed mapping of SC-FDMA

It is clear from the figure above that the localized mapping consists of "N" consecutive sub-carriers while in case of distributed mapping each set of "N" sub-carriers is separated by "L-1" zeros [13]. SC-FDMA inherently gives diversity gain over OFDM as the information data is spread over multiple sub-carriers by the DFT mapper. In comparison however the distributed mapping scheme collects more frequency diversity than the localized mapping scheme, but the pilot overhead for channel estimation is increased compared to the localized mapping scheme, LFDMA however in combination with channel dependant scheduling can offer multi-user diversity in frequency selective channel conditions [12].

In addition to LFDMA and IFDMA another mapping scheme called block interleaved FDMA or BIFDMA was introduced in [14] which is actually a generalization of IFDMA and LFDMA. Unlike IFDMA in BIFDMA equidistant blocks consisting of more than one subcarrier are assigned to users and unlike LFDMA non-consecutive sub-carriers are assigned to users [15]. If the DFT precoding step is removed before BIFDMA then it converts to block equidistant IFDMA or BEFDMA. The figure below shows the sub-carriers allocation in the three schemes

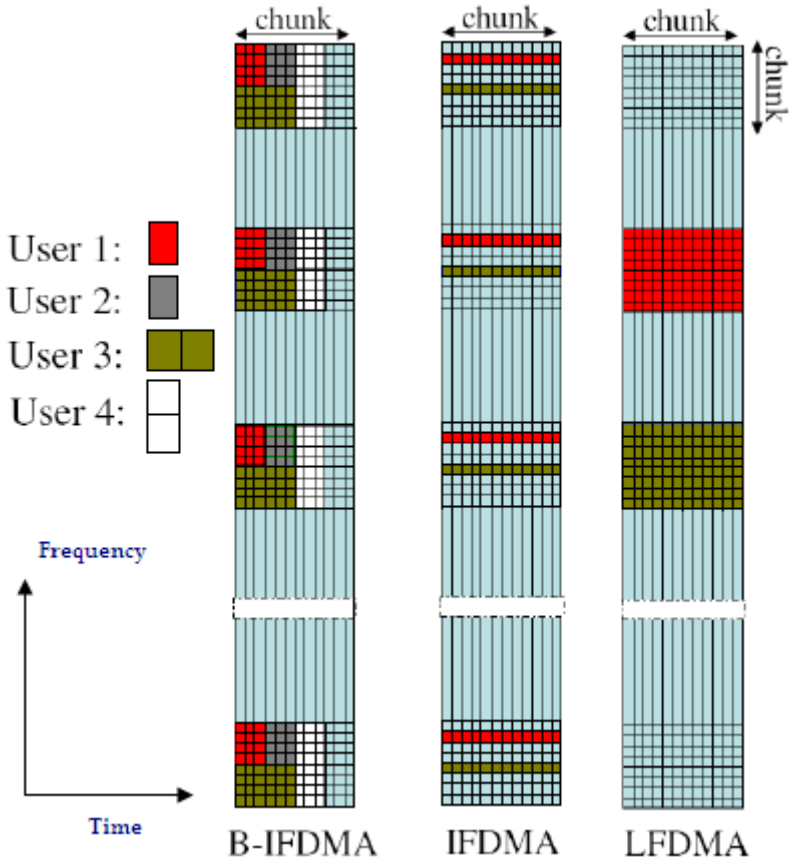

Figure 2.10: BIFDMA with 4 sub-carriers and 3 OFDM symbols per block in comparison with IFDMA and LFDMA

Here in this research study the subcarrier allocation matrix "T" is an "M×K" matrix where "M" is the total number of sub-carriers e.g. 1024 and "K" is the number of sub-carriers per user e.g. 128. The subcarrier allocation matrix in all the three cases can be given by the following equations:

IFDMA:
$$T_{IFDMA}^{(q)}(m,k)=\begin{cases}1, m=k.Q+q;\\ 0, otherwise;\end{cases} \quad (2.4)$$

LFDMA:
$$T_{LFDMA}^{(q)}(m,k)=\begin{cases}1, m=q.K+k;\\ 0, otherwise;\end{cases} \quad (2.5)$$

BIFDMA and BEFDMA:
$$T_{B-IFDMA}^{(q)}(m,k)=T_{B-EFDMA}^{(q)}(m,k)=\begin{cases}1, m=p\frac{M}{P}+l+q.L;\\ 0, otherwise;\end{cases} \quad (2.6)$$

Where "P" is the number of blocks assigned to a specific user and "L" is the number of sub-carriers per block. The index variables in the equation are m=0,…,M-1, k=0,…,K-1, p=0,…,P-1 and l=0,…,L-1.The figure below shows exactly how four sub-carriers are mapped in the three mapping schemes.

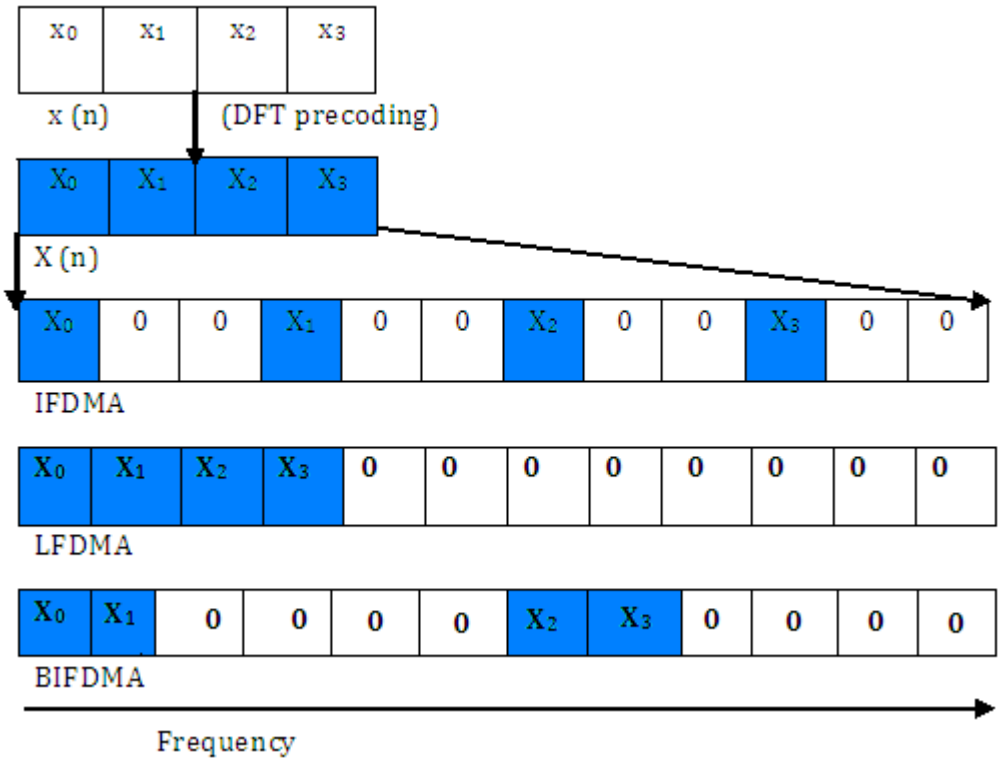

Figure 2.11: Example of mapping four sub-carriers in IFDMA, LFDMA and BIFDMA

2.2.4.1 Time Domain Representation

The symbols after being mapped are then transformed into time domain symbols by taking their IFFT on the transmitter side. Thus it is useful to study the time domain representation of the three mapping schemes. For this purpose we would use the running example that is being used in the previous figure.

2.2.4.1.1 IFDMA

The IFDMA scheme can be visualized by up-sampling a signal. The example above can be seen as equivalent to up-sampling the original DFT precoded sequence "X_n" by factor of 3 and as a result we get 2 zeros between each consecutive sample. Thus, if transformed into time domain it would give repetitions of the original time domain symbols as shown in the figure below

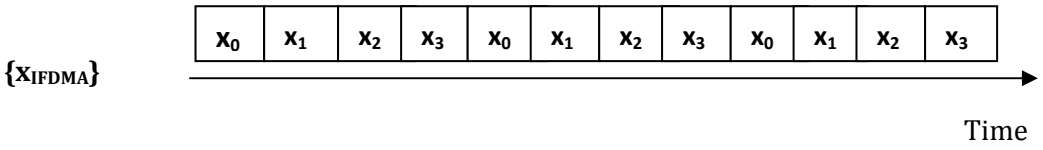

Figure 2.12: Time Domain Representation of IFDMA mapping

Hence we get "Q" repetitions of the original signal which is scaled by a factor of 1/Q where "Q" is the number of users in the system.

2.2.4.1.2 LFDMA

The figure below shows the time domain representation of LFDMA which is similar for the time domain representation of BIFDMA in our running example

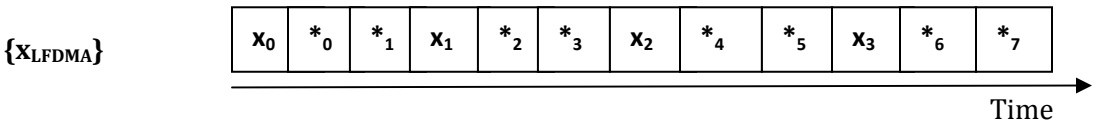

$$* = \sum_{k=0}^{3} c_{k,m}.x_k, c_{k,m} = ComplexWeight$$

Figure 2.13: Time domain representation of LFDMA mapping

Hence in LFDMA, the input symbols are repeated with a scaling factor of 1/Q at sample positions which are actually the integer multiples of "Q" where "Q" is the number of users. The values indicated by "*" are actually combinations of all the input symbols with different complex weights. It should be noted that the time domain notations for LFDMA and BIFDMA are the same in our running example, but the intermediate terms between the input symbols are different in the case of BIFDMA than in the case of LFDMA.

2.2.5 OFDM, OFDMA & SC-FDMA

With the passage of time, to accommodate increased number of users and to handle the channel conditions, different modulation schemes and multiple access techniques have been developed. The next block in the IMT-Advanced simulation model is the OFDM modulation and demodulation. In this section we discuss about the Orthogonal Frequency Division Multiplexing (OFDM), its multiuser version that is Orthogonal Frequency Division Multiple Access (OFDMA) and Single Carrier–Frequency Division Multiple Access (SC-FDMA) in combination with the Single Carrier–Frequency Domain Equalization (SC- FDE) to give our reader a brief and interesting picture of these basic terms.

2.2.5.1 OFDM and OFDMA

OFDM is a multicarrier modulation scheme that is based on frequency division multiplexing (FDM). FDM uses multiple frequencies simultaneously to transmit multiple signals in parallel. FDM and OFDM are not similar as there are few differences between them like OFDM is much more spectrally efficient by spacing the carriers or channels much closer together and saving the bandwidth by excluding the guard bands and allowing signals to overlap. FDM constitutes guard bands so it covers more bandwidth.

Another advantage of OFDM over FDM is the orthogonality of sub-carriers due to which they can be received without interference. The figure 2.14 below shows the structure of FDM and OFDM signal in frequency domain

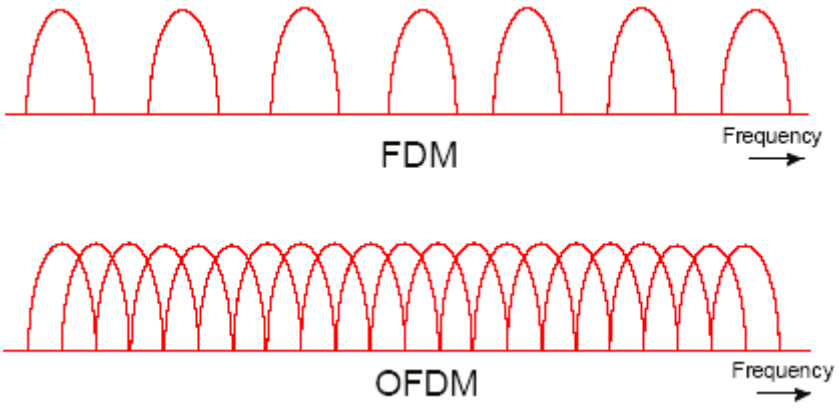

Figure 2.14: The structure of FDM and orthogonal sub-carriers in OFDM

A very important objective to bring OFDM into the game is to mitigate the fading channel effects. If a signal wants to experience flat channel then it must occupy less bandwidth than the coherence bandwidth of the channel. OFDM is a very good solution to defend the hindrances created by a fading channel as each of its sub-channels or sub-carriers experience a flat fading due to lesser bandwidth.

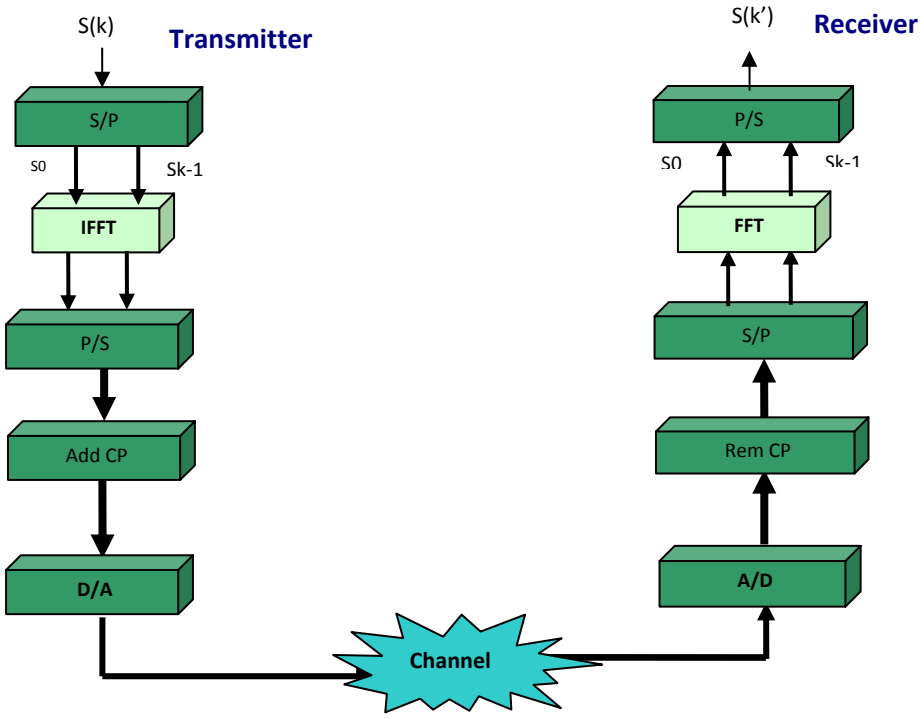

Figure 2.15: OFDM Transceiver

OFDM is also good from the time domain perspective as having slim and narrow band signals will cause the symbol duration of each one to be long enough. As symbol duration gets longer than the maximum delay spread in time, it helps to eliminate the Inter Symbol Interference (ISI) [9]. In the figure above a simple OFDM transceiver has been shown with its major blocks. The S (k) and S (k') are the modulated and demodulated symbols respectively. On the transmitter side the symbols are first converted from serial to parallel and are passed through the IFFT block that brings the signal into the time domain. After that, it is passed through the "parallel to serial" converter and finally a cyclic prefix is added to it and we get an OFDM symbol. This OFDM symbol is then sent on the channel after applying the pulse shaping (that reduces the out of band interference) and is then passed through D/A converter.

The cyclic prefix size should also be adjusted and it must be same as or greater than the delay spread of the channel so that the original information must be protected from the channel transients. On the receiver side the inverse process takes place and we get the demodulated symbol. In this simple model, there is no equalization but normally equalization is applied to mitigate the adverse effects of the channel. In OFDM, there are different types of sub-carriers; most are used to carry data. Few are used as pilot and some don't have any information and they are called null carriers. The pilot sub-carriers provides a reference to minimize frequency and phase shift during transmission and null sub-carriers serve as guard band and DC carrier [17].

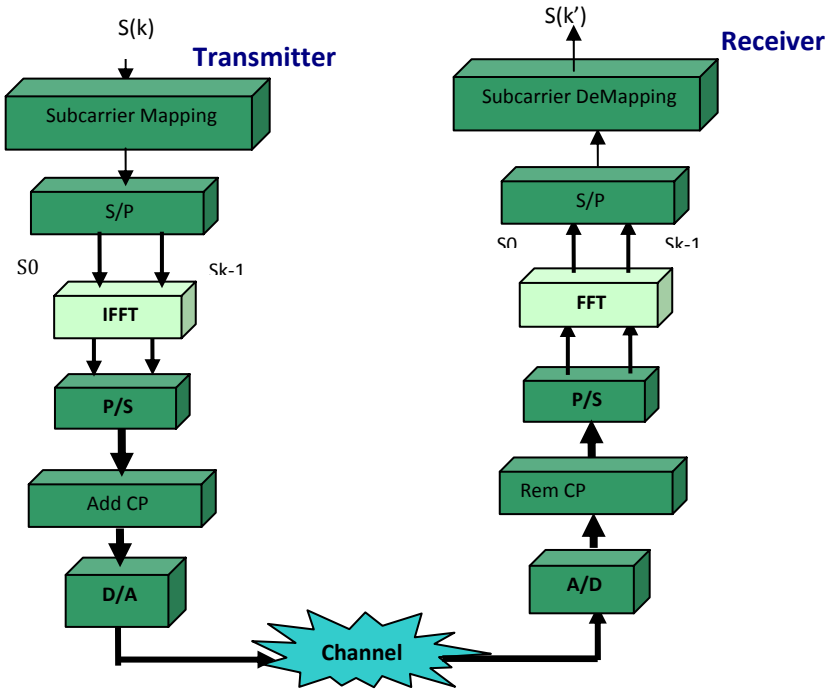

Figure 2.16: OFDMA Transceiver

The figure 2.16 above shows a typical OFDMA transceiver. The basic construction of OFDMA transceiver is almost similar but the difference comes at the carrier mapping and De-Mapping stage. OFDMA is nothing but multiple user version of OFDM. OFDMA is a multiple user access technique in which the information is sent to many users on different sub-carriers assigned to each user. This technique is used in the downlink when information is sent to a lot of users. Each user extracts the information from the sub-carriers assigned to it. In the uplink, the way how the carriers are assigned is different. In OFDM, all the sub-carriers or the full frequency band is assigned to a single user for a specific time interval. While in case of OFDMA the sub-carriers are allocated to users and

the users receive information on these sub-carriers. This technique improves not only the bandwidth utilization but also brings power gain over OFDM system in the uplink, as it allows the users to transmit only through the sub-channels that are assigned to them [17].

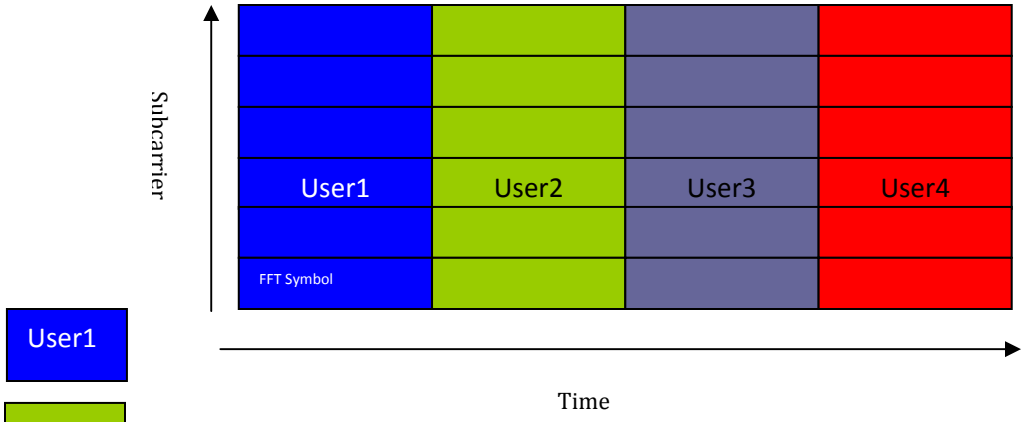

Figure 2.17: Sub-carriers in Uplink in OFDM

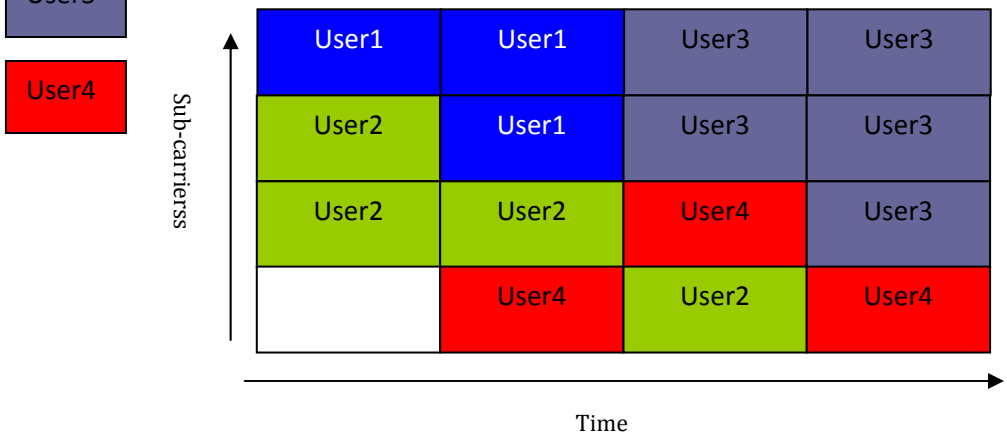

Figure 2.18: Sub-carriers in Uplink in OFDMA

In the figure 2.17 and figure 2.18, the subcarrier allocation has been shown for 4 users for OFDM and OFDMA in uplink respectively. OFDMA has many advantages like; it has brought reduction in the interference among the users as well as, has improved the Non line of sight (NLOS) communication in a mobile environment [12].

There are many advantages of OFDM like; it creates immunity against the fading and interference, provides high spectral efficiency, has no ICI due to orthognality among the sub-carriers (assuming linear environments) and is better in scenarios where channel conditions are constant. OFDMA also offers impressive features like better use of frequency resources and power gain and is suitable in the scenarios where the channel is time -

frequency selective. There are also some drawbacks of OFDM/OFDMA that are needed to be mentioned at this point of discussion. The first and major one is the high peak to average power ratio (PAPR) that is the result of superposition of all the sub-carriers with different carrier frequencies. Due to the superposition of all sub-carriers, it is very difficult to avoid high peaks of the signal. This is indicated in the figure below

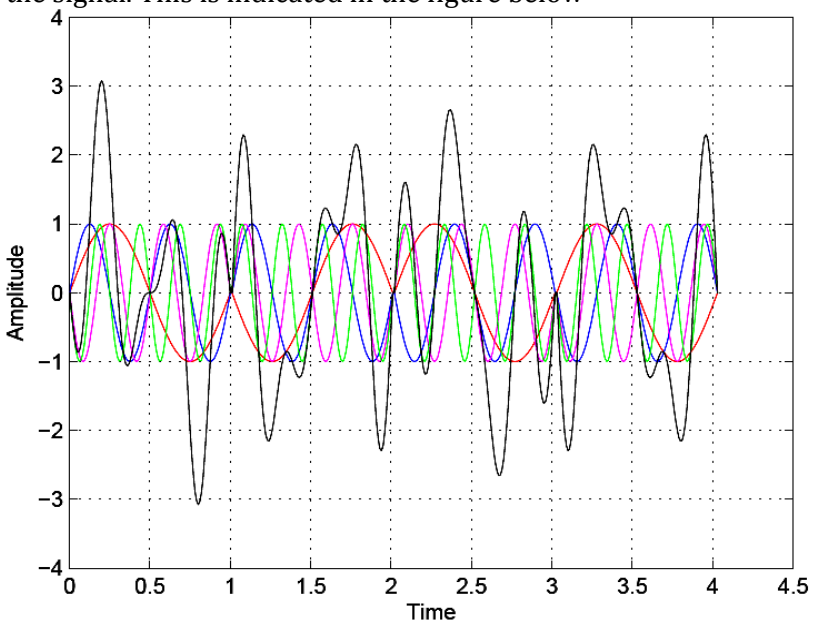

Figure 2.19: Superposition of all sub-carriers in OFDMA

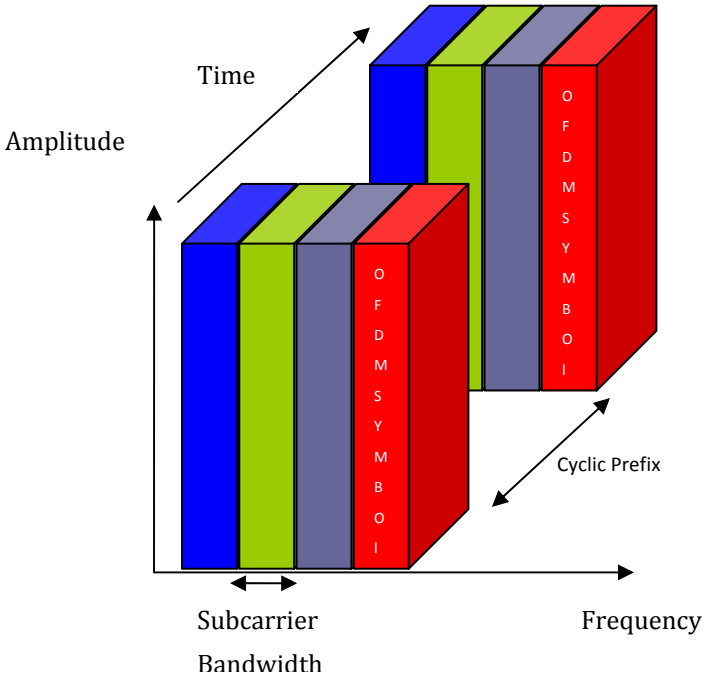

Figure 2.20: OFDM Modulation using many sub-carriers

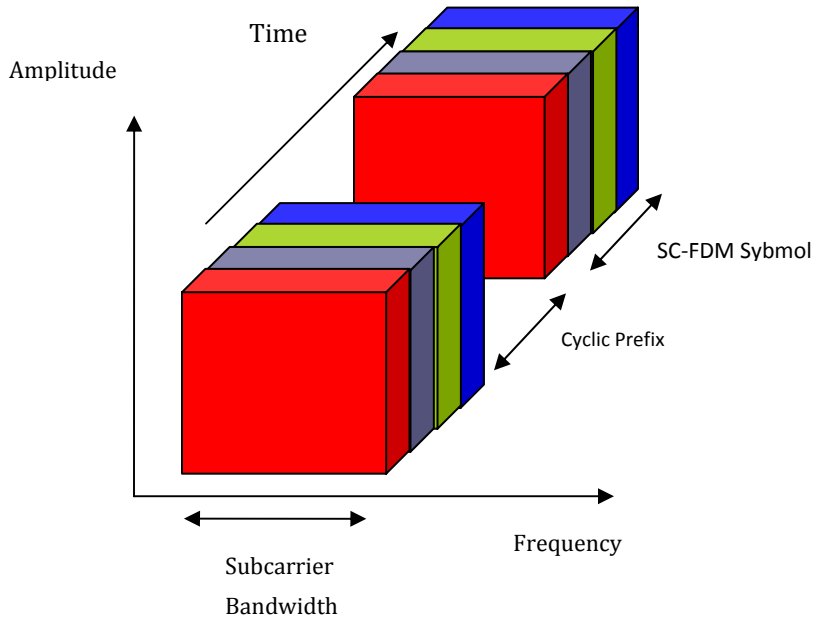

Figure 2.21: SC-FDMA using single carrier in the uplink

2.2.5.2 Advantages of Using SC-FDMA

SC-FDMA is a Single carrier-Frequency division multiple access technique that has been used in the uplink in IMT-Advanced and LTE. This modulation technique is used in combination with frequency domain equalizers (FDE) due to increased complexity of time domain equalizers. A major difference between the SC-FDMA and the OFDMA transceiver is just an addition of a DFT block on the transmitter side and IDFT detection block on the receiver side. Hence on the transmitter side, the symbols are transmitted as time domain symbols while on the receiver side, they are transformed into frequency domain symbols before equalization and after that they are detected.

The major advantage of using SC-FDE or SC-FDMA in the uplink is low PAPR ratio of the transmitted signal caused by DFT precoding done at the transmitter. PAPR is basically the ratio between the peak power to average power of the transmitted signal. PAPR is very important in relation with the amplifier efficiency at the transmitter and in the amplifier the maximum efficiency is achieved when it operates at the saturation point. The low PAPR value will allow the amplifier to operate close to the saturation region.

SC-FDMA has subcarrier bandwidth common to all sub-carriers, so there is no superposition of subcarriers like in OFDMA in figure 2.19 so the peak of the transmitted signal is not so high. Interleaved SC-FDMA is a preferred modulation technique for lower PAPR. Pulse shape filtering of SC-FDMA in fact degrades the PAPR level of interleaved SC-FDMA whereas it shows no effect with localized SC-FDMA [12]. Now if we look at figure 2.20 and figure 2.21 we can see that SC-FDMA uses the whole bandwidth for each symbol in the frequency domain hence, it is more immune to frequency selective fading. But in time domain it is very short and will face more ISI as compared to OFDMA. So it becomes necessary for SC-FDMA to use an equalizer to mitigate the ISI effects [9].

2.2.6 NON-LINEAR AMPLIFIERS

It is a well known fact that OFDM comprises of large envelope fluctuations as compared to single carrier systems with same modulation and same spectral characteristics. This is because OFDM is nothing but sum of multitude of digitally modulated signals with Gaussian like probability density function (PDF). Hence the peak to average power ratio (PAPR) of OFDM is quite large which results in an inefficient usage of the high power amplifier (HPA) at the transmitter [18]. The high PAPR causes the HPA to enter into the non-linear region and thus we get distortions due to non-linearities at the output of the HPA. Normally non-linear regions are prevented by "backing off" the amplifier from the saturation region thus keeping it in the active or linear region of operation. This backoff would however affect the efficiency of the HPA. Hence it is desired to maintain low back off values but this would cause an additional interference as non-linear distortions and peak value limitations produced as a result would result in inter-modulation between different carriers [19]. It is thus desired to keep the back off values low but at the same time prevent the non-linearities caused by the HPA.

2.2.6.1 Amplifier characteristics

To better understand the impact of non-linearities on our multicarrier modulated signal it is useful to study briefly the basics of a bipolar junction transistor (BJT) amplifier. A BJT basically consists of three alternatively doped semiconductor regions and two PN junctions. The three layers are called emitter, base and collector and the junction between emitter and base is the emitter base junction while the junction between collector and base is called the collector base junction.

For normal operation of the BJT the emitter base junction is forward biased and the collector base junction is reverse biased. There are four different modes of operations of a BJT which are briefly explained below:

2.2.6.1.1 Cut off region

In the cutoff region both the emitter base junction and the collector base junctions are reverse biased and hence there is a negligible current flow due to minority carriers. Hence the amplifier is essentially in "OFF" state.

2.2.6.1.2 Saturation region

If both the PN junctions of the BJT amplifier are forward biased, it will be in saturation region of its operation. The saturation region operation is opposite of the cutoff region operation and is essentially a logical "ON" state. The collector emitter current in the saturation region reaches a maximum which is independent of the base current [20].

2.2.6.1.3 Active region

In this case the emitter base junction is forward biased while the collector base junction is reverse biased and the output collector emitter current increases as a function of the base current in this region. Moreover the collector emitter current has a very small slope with V_{CE} [20].

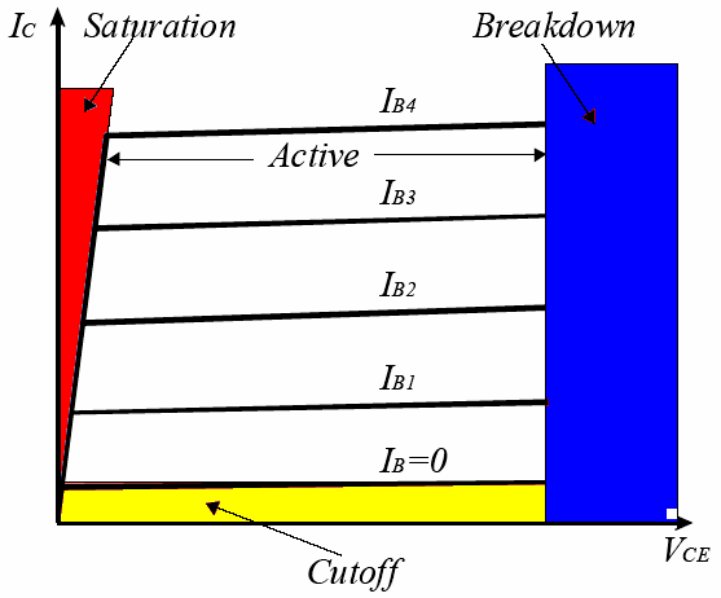

Figure 2.22: BJT IV characteristics curve

2.2.6.1.4 Breakdown region

In the breakdown region the input collector to emitter voltage would increase beyond the breakdown value as a result of which the transistor breaks down with a tremendous increase in the collector emitter current. The figure 2.22 shows IV characteristics of a typical BJT indicating the four regions of its operations that are mentioned above.

2.2.6.2 Non-linearity Modeling

Non-linearities in multicarrier systems can be modeled in many different ways. Some of the techniques used for modeling HPA non-linearities are travelling wave tube (TWT) amplifier with strong AM/PM conversion, solid state amplifier (SSA) model and idealized amplifier model called "envelope limiter" (LIM) [19]. For our analysis in this thesis we use non-linear amplifier at the transmitter side and we implement it using simple non-linear distortion-clipping or soft limiter (SL). However the same analysis can be applied to more sophisticated non-linear amplifiers. The clipped outputs $x^c(n)$ of our time domain signals x(n) are given by

$$x^c(n) = \begin{cases} x(n), & |x(n)| \le A \\ Ae^{i\arg\{x(n)\}}, & |x(n)| > A \end{cases} \qquad (2.7)$$

Where A is the clipping threshold [21].

The figure below shows a typical threshold clipper with threshold value equal to A=500.

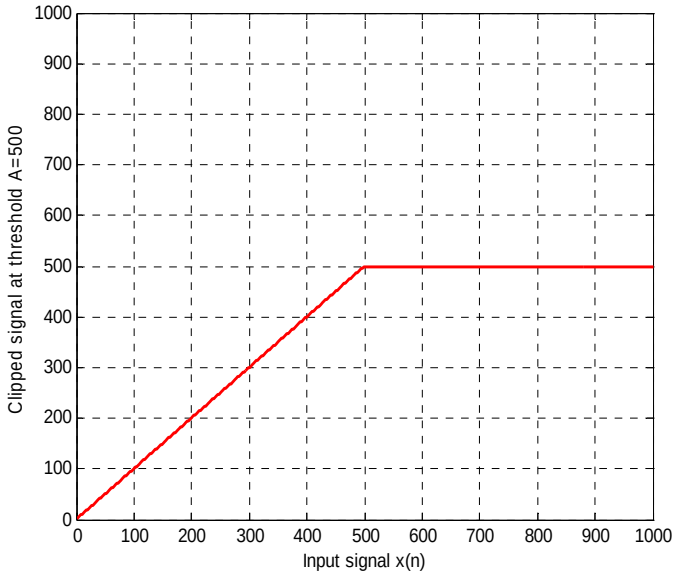

Figure 2.23: Threshold clipping for Non-linearities modeling

2.2.6.3 System degradation by HPA Non-linearity

The distortions produced by a non-linear amplifier are dependent on envelope fluctuations. A non constant envelope signal when modulated by a non-linear amplifier would be distorted in different ways. The non-linearities in the HPA would cause additional interference in the receiver. We would get interference between the in-phase and quadrature components due the AM/PM conversion. Moreover the power spectral density (PSD) of the modulated signal with fluctuating envelope would be broadened by the non-linear effects of the HPA that would cause spectral spreading of the signal and hence adjacent channel interference would be introduced in the amplifier output. Finally it should be noted that when several channels are amplified in the same HPA, there would be inter-modulation effects in the amplifier output signal. In other words the orthognality in OFDM would be completely destroyed by the non-linear distortions in the HPA [19].

As mentioned earlier one way of preventing these effects is to make the amplifier operate in the linear region which would require introduction of "output back off" (OBO) of the HPA which is given by

$$OBO = 10\log_{10}(\frac{P_o}{P_s}) \text{ in dBs} \qquad (2.8)$$

Where the reference power "Po" is the saturating power of HPA and "Ps" is the mean output power of the transmitted signal. It is however unfortunate that the efficiency of the HPA is very low at high values of OBO so there is a tradeoff between maximizing output power on one side and avoiding degradations due to non-linear distortions on the other side [19].

2.2.6.4 Power Control in Uplink

In this part of the report we discuss the role of power control in the LTE uplink and its mathematics followed by its types.

2.2.6.4.1 Power Consumption

As discussed already, power consumption is a key factor when we are dealing with the LTE uplink. The user equipment (UE) is actually energy limited by its energy source usually a battery. The SC-FDMA approach mentioned earlier is actually intended to keep the PAPR to a lower level. Power control in uplink can also be seen as a method to save

unwanted power consumption in the user equipment (UE) and hence increasing the battery life [22].

2.2.6.4.2 Inter and Intra Cell interference

Secondly the SC-FDMA signals from different UEs are orthogonal and hence they do not interfere at the receiver in ideal circumstances but in practice the orthognality is disturbed by certain impairments in transmitter and receiver. These transmitter imperfections would cause the signals from different UEs to leak beyond their intended frequency bands and interfere with each other. The transmitter impairments can be expressed by the Inband Subcarrier Set Leakage (ISSL) which describes the allowed disturbance from one UE transmitter located on one subcarrier set onto another subcarrier set within the regulatory bandwidth of the UE. ISSL is thus a measure of the leakage between the sub-carriers. It should be noted that ISSL of about 25dBs or more seems reasonable to achieve [23]. The figure below shows a typical received PSD affected by transmitter impairment with an ISSL of 25dBs

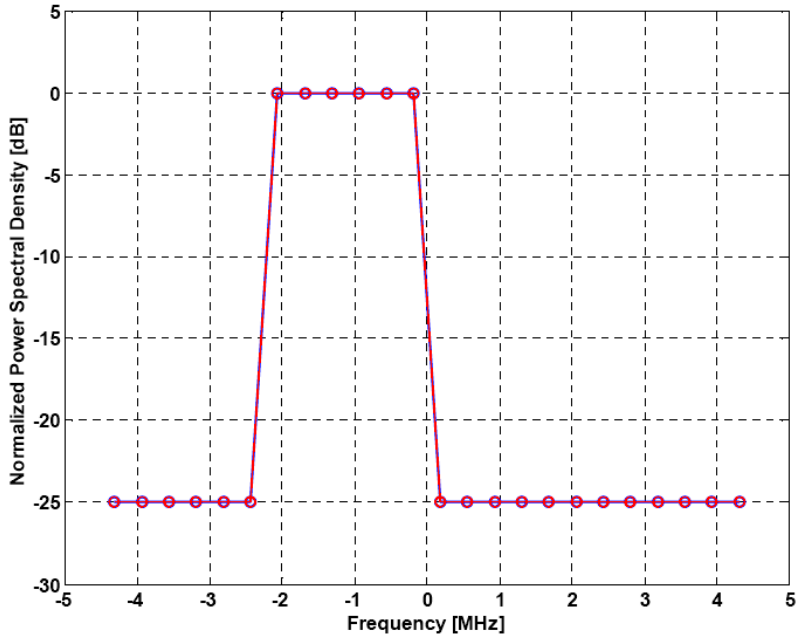

Figure 2.24: Transmitter imperfection model: PSD with ISSL=25dBs

The transmitter impairments may include phase noise or IQ imbalance. Moreover, the HPA non-linearities being discussed earlier in this chapter is also one of the transmitter impairments that would cause leakage between sub-carriers assigned to different UEs (intra cell multiple access interference). In addition to intra-cell interference due to

transmitter and receiver impairments there can be interference from the neighboring cells which is called inter cell interference and which can limit the system performance in terms of its capacity [24]. These forms of interference can be controlled by a power control scheme which would essentially control the received PSDs and would restrict the signals to their desired frequency bands [25].

2.2.6.4.3 Power control Equation

Power control is a technique that varies the radio-link transmit power in accordance with the instantaneous variations in the channel conditions. In simple words the transmit power control would increase the transmit power when the radio link experiences poor radio conditions and would reduce power in case of good radio conditions. Hence the transmit power is essentially inverse of the channel quality [2]. The agreed upon power control formula for LTE uplink is

$$P = \min\{P_{\max}, 10.\log_{10} M + P_o + \beta.P_L + \delta_{mcs} + f(\Delta_i)\} \quad \text{[dBm]} \qquad (2.9)$$

Where

- $P_{\max}$ is the maximum power allowed and it depends on the UE power class.
- M is the number of physical resource blocks (PRBs).
- P_o is cell/UE specific parameter signaled by radio resource control (RRC).
- It is measured in dBm and represents power contained in one PRB.
- β is path loss compensation factor with values ranging between 0 to 1.
- PL is the downlink path loss estimate at the UE.
- δ_{mcs} is cell/UE specific modulation and coding scheme.
- $f(\Delta_i)$ is UE specific and it permits to use absolute or accumulate correction value.
- P_o in the above equation can be calculated as

$$P_o = \beta.(SNR_o + P_n) + (1-\beta)(P_{\max} - 10.\log_{10} M_o) \text{ [dBm]} \qquad (2.10)$$

Where

- SNR_o is the open loop SNR target.
- P_n is the noise power per PRB.
- M_o is the number of PRBs for which the target SNR is achieved with full power [24].

The parameters " P_o " and "β" are broadcast by the base station (also called evolved node B (eNB) in 3GPP terms) to all the UEs and together with path loss are sufficient to set initial transmit power. These are thus called open loop terms. The "δ_{mcs}" and "Δ_i" are however signaled to UE as its grant from the eNB after the initial power has been set according to open loop terms and feedback is sent to eNB.

These are thus called the closed loop terms [26]. The power control equation given above can be simplified by neglecting the unnecessary terms to get the simplified equation given below

$$P = P_o + \beta.P_L \text{ [dBm/PRB]} \quad (2.11)$$

2.2.6.4.4 Types of Power control

Based on speed of channel variation power control is of two types

- Slow Power Control: Designed to compensate for slow channel variations.
- Fast Power Control: Designed to compensate for fast channel variations.

Based on the type of information sent to the UE to adjust its transmit power, power control is of two types

- Open Loop Power Control: The transmit power is measured at the UE using the open loop parameters sent by the eNB and no information is sent to eNB.
- Closed Loop Power Control: The UE send feedback to the eNB in this kind of method to correct its transmit power value [26].

Based on the value of β we have three types of power control schemes

- No Path Loss Compensation: When β is 0 we won't have any power control and all users would use maximum allowed transmission power.
- Fractional Path Loss Compensation: For 0< β <1 the type of power control is called fractional power control scheme as it compensates fraction of the path loss. Since Po and β are same for all UEs so it's the path loss PL which would make each user to be received with different values of PSDs.
- Conventional Path Loss Compensation: When β=1 the power control scheme is called conventional power control scheme as it compensates for the whole of path loss. This scheme would essentially equalize the power of all UEs before

being received at the eNB and thus has an advantage of eliminating the near far problem as of typical CDMA systems [24].

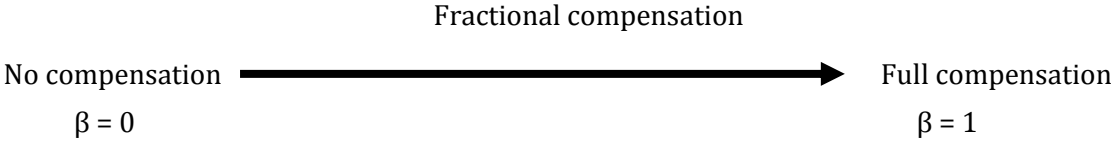

Figure 2.25: Power control schemes based on values of β

2.2.7 Channel & Equalization

In this part of the text we have discussed about the key channel characteristics and later on the equalization methods to reduce the effects of the channel impairments.

2.2.7.1 Channel Characteristics

The wireless channel consists of many severe challenges like noise, interference and many other impairments that effect mobile communication over time and frequency due to the high mobility of users. We have discussed some key impairment in general that affect the wireless communication signal.

2.2.7.1.1 Path Loss

Path loss is one of the channel characteristics that is caused by dissipation of the power radiated by the transmitter as well as effects of the propagation channel. There are different path loss models including the free path loss and empirical path loss models that describe the path loss. In case of free space model no obstructions are considered in between the transmitter and receiver and the propagation is assumed to be line of sight (LOS). The channel model associated with this transmission is called a line-of-sight (LOS) channel, and the corresponding received signal is called the LOS signal or ray [1].

Let P_t be the transmitted power of the signal and let P_r be the received power of the signal then path loss P_L is defined as,

$$P_L = \frac{P_t}{P_r} \tag{2.11}$$

While the path loss can also be defined as in dB,

$$P_L dB = 10 \log_{10} \frac{P_t}{P_r} dB \tag{2.12}$$

The modern day complex mobile environments cannot be modeled by using simple free space path loss models so some more complex models that are more near to mobile

communication environments are required. The empirical models are one of them that are used to predict path loss in typical wireless environments such as large urban macrocells, urban microcells, with more distance in a given frequency range and a particular geographical area or building. The examples of such kind of models are the Okumura Model and Hata Model [1].

2.2.7.1.2 Shadow Fading

A signal that is transmitted through a wireless channel experiences different random variations due to the hurdles and different obstructions or objects in the environments that comes in the signal path. Such variations are also caused by changes in reflecting surfaces and scattering objects and they result in the variation of power of received signal. This type of effect on the received power is called shadowing or shadow fading. Here in the figure below we can see the combined effect of the three different factors that causes variation in signal strength.

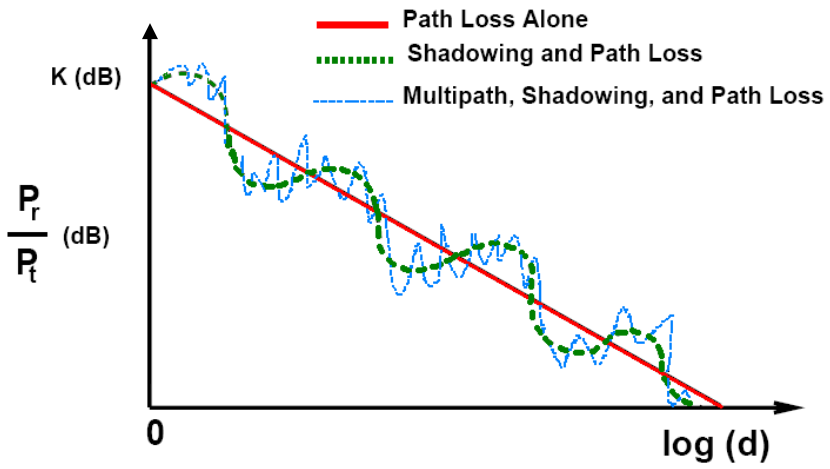

Figure 2.26: Combined Path loss, shadowing and multipath propagation effect

2.2.7.1.3 Narrow band fading

Before moving to narrow band fading here we would like to discuss briefly about multipath propagation that creates ISI at the receiver. The Multipath propagation results due to the multiple copies of the same signal coming from different paths at the receiver with different delays in time. The multiple copies are also called multi path components.

Here it is also necessary to mention about the delay spread that is the time difference between the arrival of the 1st multipath component and the last multipath component of the transmitted signal. This is denoted by "Tm". There is a difference between the delay spread and Doppler spread. The Doppler spread occurs due to the Doppler shift and the Doppler shift is basically the change of frequency of wave as observed by the receiver when it is moving toward or away from the source with some velocity [9].

When many multipath components are generated then due to the constructive and destructive addition of multipath signal components, the received signal strength varies very rapidly over a small distance usually in the order of signal wavelength. Since the propagation channel varies over small distance it is called small scale fading. Small scale fading has been modeled as random time varying impulse response.

Narrow band fading is one of the types of the small scale fading that results from the multipath propagation and is based upon the relationship between signal bandwidth and maximum delay spread of the channel and it fulfills this relation $Tm << B^{-1}$.

"Tm" is the delay spread while "B" is the bandwidth of the transmitted signal. So this means that in narrow band fading the delay spread or the difference between the delays of multipath components will be very small as compared to the bandwidth of the signal. Narrowband fading can be modeled practically by Clarke's or Jake's model that assumes that all the multipath components arrive uniformly with same average power and with same angle of arrival [9].

2.2.7.2 Wideband fading

This is another type of small scale fading where we observe distortion due to multipath delay spread when the signal bandwidth is approximately equal to inverse of delay spread $B \approx 1/T_m$. In the wideband fading the delay in between the multipath components is much lower than the narrow band fading. This results in longer duration of received pulses that creates interferences with the neighbor pulses thus causing the ISI. OFDM is a kind of mitigation technique that is used to change the characteristics of the transmitted signal by extending the symbol duration mainly to overcome ISI [9]. The Wideband channels are usually characterized by time-varying impulse response and time-varying frequency response. Time-varying impulse response $c(\tau ; t)$ is modeled as a two-dimensional random process and time-varying frequency response $C(f; t)$ is obtained from

$c(\tau ; t)$ by taking the Fourier transform with respect to τ i.e., $C(f; t) = F_{\tau}[c(\tau ; t)]$. An example of a two-dimensional discrete-time varying impulse response $c(\tau ; t)$ is shown in the figure below [9].

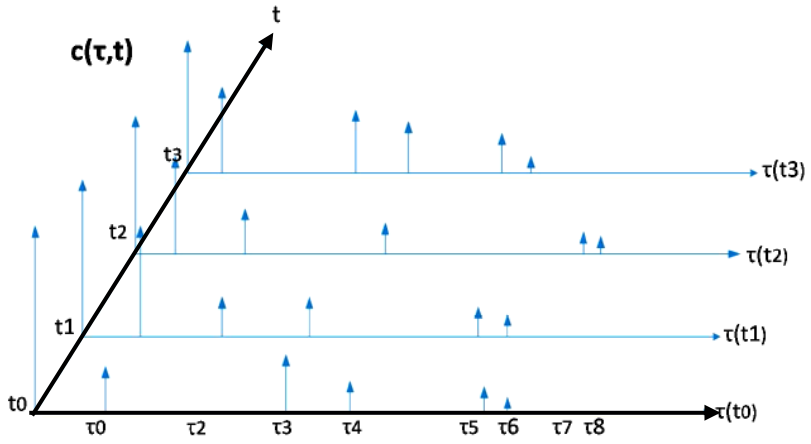

Figure 2.27: Time-Varying Discrete-Time Impulse Response Model for a Multi-Path Channel

In the following some key properties of a wideband fading channel has been discussed including the power delay profile, coherence bandwidth, and Doppler power spectrum. These characteristics are based on channel autocorrelation or scattering function.

2.2.7.2.1 Power Delay Profile

Power delay profile (PDP) is one of the important characteristics of wideband fading. The PDP represents the average power of each multipath delay component. The PDP basically shows the strength of multipath components and their corresponding delays in the channel so it is also referred to as multipath intensity profile. It is important to mention here about the channel delay spread that can be either average delay spread (μ_{Tm}) or the root mean square (RMS) delay spread (σ_{Tm}). Both of them can be analyzed from the power delay profile.

$$\mu_{Tm} = \frac{\int_0^{\infty} \tau Ac(\tau)}{\int_0^{\infty} Ac(\tau)}, \sigma_{Tm} = \sqrt{\frac{\int_0^{\infty} ((\tau - \mu_{Tm})^2 A_c(\tau))}{\int_0^{\infty} Ac(\tau)}} \qquad (2.13)$$

The power delay profile of the WINNER-C2 NLOS can be seen shown below,

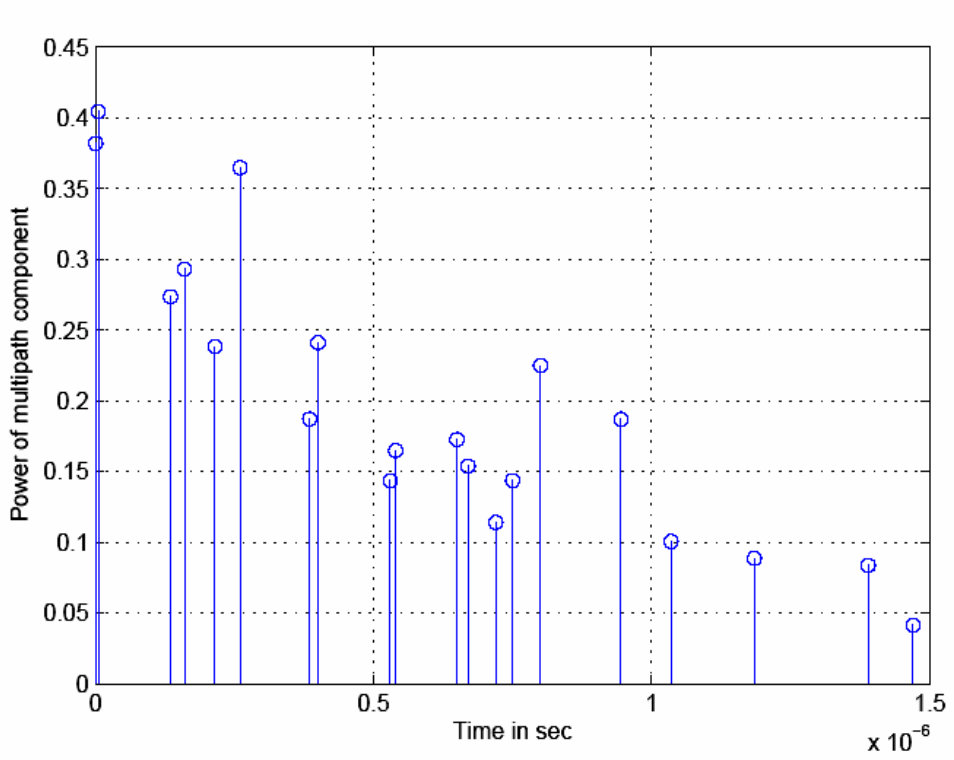

Figure 2.28: Normalized Power Delay Profile of WINNER–C2 NLOS

We can describe the delay spread as the maximum delay "Tm" after which the power of all multipath components becomes negligible. The PDP can be used to assess whether the system has ISI or not. In the channels that have many scatterers the delay spread is approximately equal to the RMS delay spread.

2.2.7.2.2 Coherence bandwidth

The coherence bandwidth "Bc" according to [1] is where $A_c(\Delta f) \approx 0$ for all $\Delta f > B_c$. Coherence bandwidth is actually the range of frequencies over which the channel passes all spectral components with almost equal gain and linear phase [9]. It is also the band of frequencies over which the channel is highly correlated in frequency. There is a high relationship between the fading and the coherence bandwidth of the channel. If the bandwidth of the signal is much less than the coherence bandwidth, then this signal is going to experience fading equal over its entire bandwidth and this type of fading is called flat

fading. If the bandwidth of the signal is more than the coherence bandwidth of the signal then the signal will experience frequency selective fading.

2.2.7.2.3 Doppler Power Spectrum & Coherence Bandwidth

Doppler power spectrum is also one of the important characteristics of the wideband fading. The Doppler power spectrum basically describes the variations of the channel which occur due to the movement of transmitter or the movement of receiver. As the transmitter or the receiver moves rapidly there is a change or shift in the frequency of the received signal that is called the Doppler shift. This Doppler Effect can be measured by taking the Fourier transform of the autocorrelation Ac ($\Delta f ; \Delta t)$) with respect to " Δt " so $Sc(\Delta f ; \rho) = F_{\Delta t}[Ac(\Delta f ; \Delta t)].Sc(\rho) \overset{\Delta}{=} Sc(0; \rho)$ characterizes Doppler shift for a single frequency and $Ac(\Delta t) \overset{\Delta}{=} Ac(\Delta f = 0; \Delta t)$ describes the behavior of the autocorrelation function with time and is used in defining the Coherence time [1]. The coherence time "Tc" describes how the channel de-correlates over time. It defines the range of values over which Ac (Δt) is approximately non-zero. The fast or the slow fading depends on the coherence time. If the symbol duration is very small as compared to the coherence time (Ts<<Tc) then the channel impulse response would be time invariant over one symbol period and this type of fading is called slow fading while on other hand if Tc<<Ts then the Impulse response varies over one symbol period and the fading is known as Fast fading.

2.2.7.3 Channel Equalization

Equalization is a technique that is used to recover the signal by mitigating the adverse effects of the channel. The basic objective of the equalizer is to typically balance ISI mitigation with noise enhancement. There are various types of the equalizers including linear and non-linear equalizers. The non-linear equalizers suffer less from noise enhancement than linear equalizers, but they are more complex. Equalizers estimate the channel impulse or frequency response to mitigate the resulting ISI. As the wireless channel varies over time, then the equalizer must also discover the frequency or impulse response of the channel (training) and then update its estimate of the frequency response as the channel changes (tracking) [1]. This type of process in which the equalizers adopt them self with the change of channel by training and tracking process is often called as adaptive equalization, as the equalizers adapt to the changing channels. The process of the

equalization might be very different and the process of tracking and training becomes complex when the channel is changing rapidly.

An equalizer can be implemented at baseband, Radio Frequencies (RF), or IF. Most equalizers are implemented digitally after A/D conversion, since such filters are small, cheap, easily tunable, and very power efficient [1]. The OFDM symbol, with flat fading experienced by each of its sub-carriers, offers an advantage in equalization. This is because; a single tap equalizer can be used for compensation. A single tap equalizer is nothing but a simple delay-line meaning that a previous detected symbol can be used for equalization of flat fading channels.

There are different types of equalizers but in this thesis project we have used an MMSE equalizer. In MMSE equalization the goal of the equalizer design is to minimize the average mean square error (MSE) between the transmitted symbol and its estimate at the output of the equalizer. Here is the equation that describes the parameters of an MMSE equalizer

$$C_{MMSE} = \frac{H^H}{|H|^2 + \frac{\sigma_w^2}{\sigma_s^2}} \tag{2.14}$$

Chapter 3

SIMULATIONS & RESULTS

In this chapter we describe the simulations parameters as well as the results acquired from these simulations that are based upon different cases related to performance analysis of Turbo coding.

3.1 System Specifications

The basic system that is being simulated looks like the one shown earlier in figure 2.2. Here we try to present the signal flow from the transmitter to receiver and the dimensions of each block used to process the signal. All the signals are represented by their discrete time equivalents in the complex baseband. The matrices are represented by capital letters while the vectors are represented by small letters. Super-scripts and sub-scripts are used to indicate the number of users and the number of sub-carriers related to each signal respectively. $(.)^{T}$, $(.)^{H}$ and $(.)^{\dagger}$ are used to represent transpose, hermition and pseudo inverse respectively.

A system having "Q" users is considered throughout the derivation with the user index "q" ranging from 0, 1..., Q-1. Raw data for each user is represented by *"$d^{(q)}$"*. The data from each user is first encoded by the Turbo encoder and the coded bits in one chunk duration are fed into the QPSK modulator. The energy of each modulated symbol is normalized to make it equal to unity. The modulated symbol for each user is denoted by *"$s_K^{(q)}$"* where "K" is the number of sub-carriers assigned to a user.

In the DFT precoded linear system the modulated symbols are converted into frequency domain by taking a K-point FFT. The DFT precoding matrix is a K×K matrix denoted by *"F_k"*. The DFT precoded symbols are them mapped to "K" out of "M" sub-carriers by the subcarrier mapping matrix denoted by *"$T^{(q)}$"* which is an M×K matrix. The matrix *"$T^{(q)}$"* can take any of the form mentioned earlier in the report in equations 2.4, 2.5 and 2.6 depending on the type of subcarrier mapping scheme being used. M-point IFFT of the signal is then taken and cyclic prefix of suitable length is added. The signal is then transmitted over the channel. The channel being used is the WINNER-C2 NLOS whose multipath propagation channel coefficient matrix for q^{th} user is denoted by "$H^{(q)}$". The signal is also corrupted by AWGN "W_M" as it is passed through the channel. The mathematical representation of received signal in DFT precoded system is thus given as

$$r_M^{(q)} = H^{(q)}.F_M^H.T^{(q)}.F_k.s_k^{(q)} + W_M \qquad (3.1)$$

The process in the non DFT precoded linear system is the same except that the DFT precoding matrix "F_k" in equation 3.1 is not used. This implies that in non DFT system the modulated symbols can be seen as time domain symbols unlike in DFT precoded where they are in frequency domain.

The mathematical representation of the received signal in a non-DFT precoded system is given below

$$r_M^{(q)} = H^{(q)}.F_M^H.T^{(q)}.s_k^{(q)} + W_M \quad (3.2)$$

In the non-linear system a threshold clipper is added into the system which is seen shaded in the figure 2.2. This makes the system non-linear by clipping the signal above a certain pre-determined threshold. Moreover it is worth mentioning that the cyclic prefix and the clipping are not included in the mathematical equations. This is because cyclic prefix is just addition and subtraction of some bits and has no real impact on the mathematical modeling of the system as far as its length is greater than or equal to the delay spread of the channel [9]. The clipping on the other hand will change the mathematical modeling of the system and can be approximated by mathematical models but they are ignored since they are outside the scope of this thesis.

One the receiver side the cyclic prefix is first removed which is followed by taking an M-point FFT. This is followed by subcarrier demapping. The subcarrier demapping matrix *"$T^{(q)\dagger}$"* is a K×M matrix and is pseudo inverse of the subcarrier mapping matrix *"$T^{(q)}$"*. The adverse effects of the channel are mitigated by using an equalizer. The equalizer being used in this thesis is MMSE frequency domain equalizer (FDE). The equalizer coefficient matrix is represented by a K×K diagonal matrix denoted by $C^{(q)}$. This is followed by DFT pre-decoding the signal if DFT precoding has been employed at the transmitter. Then the received signal is demodulated and decoded to get estimates of the transmitted bits. The mathematical representation of the received signal being processed at the receiver is given below

$$\hat{S}_k^{(q)} = F_k^H.C^{(q)}.T^{(q)\dagger}.F_M.r_M^{(q)} \quad (3.3)$$

For non DFT precoded system the equation remains the same with the removal of the DFT pre-decoding matrix "F^H_K".

$$\hat{S}_k^{(q)} = C^{(q)}.T^{(q)\dagger}.F_M.r_M^{(q)} \quad (3.4)$$

The table below shows the simulation parameters of the simulated system,

Bandwidth	80MHz
Carrier Frequency	3.7GHz
Sampling Frequency	1/12.5ns
Sampling Time	12.5ns
Guard Interval	1.47ns
Total Number of SCs (M)	1024
No of SCs per User (K)	128
SCs per Block (BIFDMA Only)	4
Chunk Width	12
Modulation	QPSK
Coding	Turbo Coding, Code rate ½, [G1,G2]=[11111,10001]
Equalizer	MMSE
Channel Estimation	Perfect
Channel	WINNER-C2 NLOS User Velocity=50 Km/h Coherence Bandwidth=680.27 KHz Coherence Time=5.8 ms

Table 3.1: Simulation Parameters

3.2 Delimitations

The cases with amplifier non-linearities have been analyzed excluding the IFDMA mapping scheme. The reason behind this is that we have not used pulse shaping in this thesis. At a later point in the thesis it was realized that IFDMA mapped signal cannot be clipped with the clipping method that we have employed. In our "threshold clipper" the absolute value of the input signal to the threshold clipper is first sorted to find the appropriate clipping threshold which is then used to clip the original input signal to the threshold clipper. In case of IFDMA however if we observe its time domain representation as shown in figure 2.12, it's nothing but "Q" repetitions of the original signal scaled by a factor 1/Q. Thus sorting it and then clipping it will not clip the IFDMA signal by the percentage intended but would rather clip each repetition by some amount which is not what is required. A more practical approach for analyzing IFDMA in non-linear environments will be to include pulse shaping in the simulations which we have not included due to time constraints in this thesis.

3.3 AWGN & Rayleigh Fading Channel

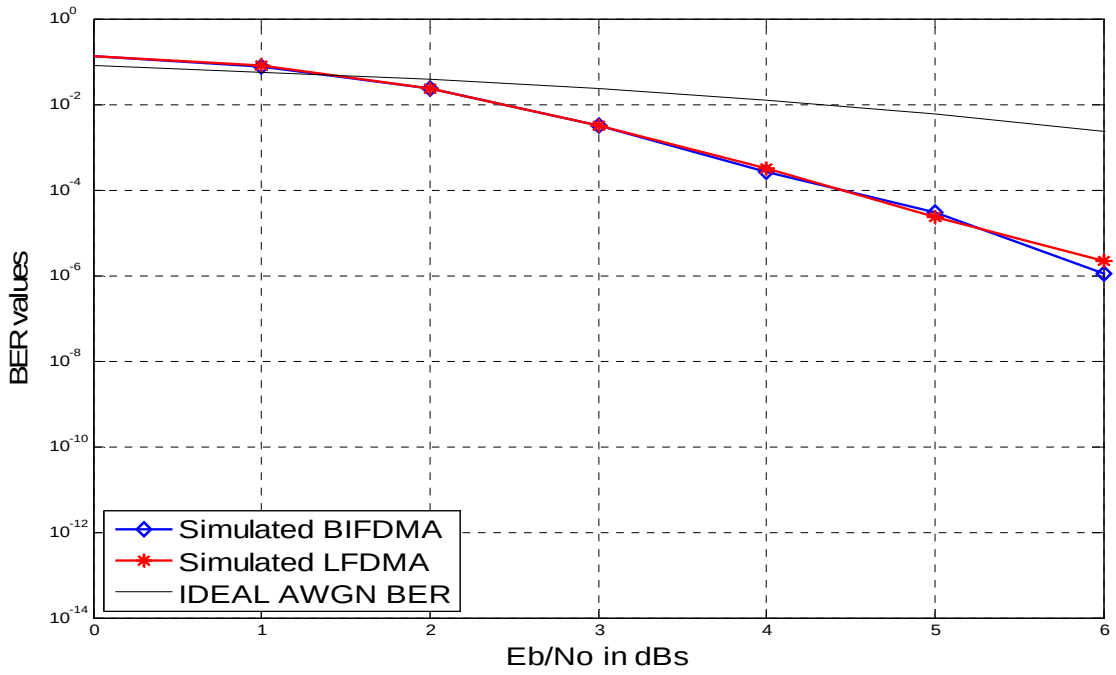

Figure 3.1: BIFDMA & LFDMA Performance on AWGN Channel
With respect to Turbo [Iterations=1]

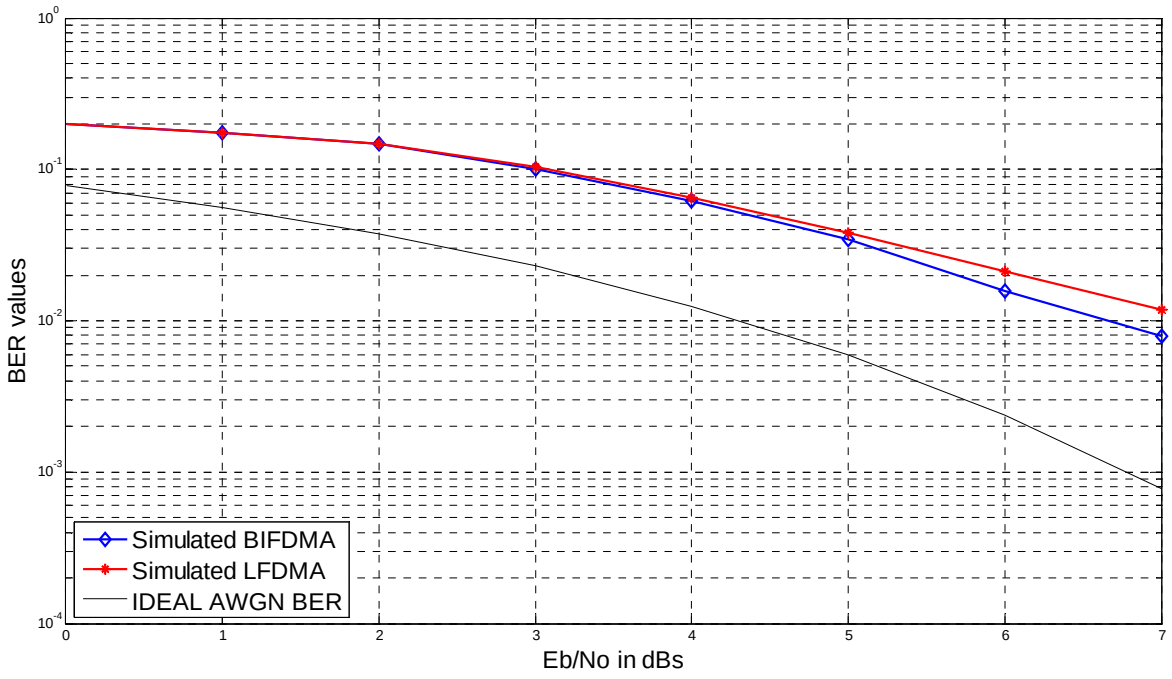

Figure 3.2: BIFDMA & LFDMA Performance on Rayleigh Fading Channel
With respect to Turbo [Iterations=1]

Figures 3.1 and 3.2 above show the performance of Turbo codes over AWGN and Fading channel respectively with 1% clipping. As expected the performance with AWGN channel is better than with fading channel. The performance of both BIFDMA and LFDMA on AWGN channel is similar with some deviations above approximately 4dBs. The reason is that both the schemes collect the same frequency diversity over AWGN channel with no fading, while the deviations are a result of the inter-user interference caused by the non-linearities which would cause the power from one user to leak into the other user. Here 1% clipping means clipping only 10 samples out of total 1024 samples which will result in very small deviations as seen in both the above figures. Considering the Rayleigh Fading channel the BER is higher for LFDMA beyond 5dBs due to the increased frequency diversity collected by BIFDMA compared to LFDMA. Moreover BIFDMA is more robust against amplifier non-linearities due to relatively small envelope fluctuations compared to the LFDMA scheme [10].

3.4 Performance evaluation of Turbo Coding

In this section we analyze the performance of Turbo code over Rayleigh Fading Channel in Linear environments with single user and multi-users.

3.4.1 SINGLE USER

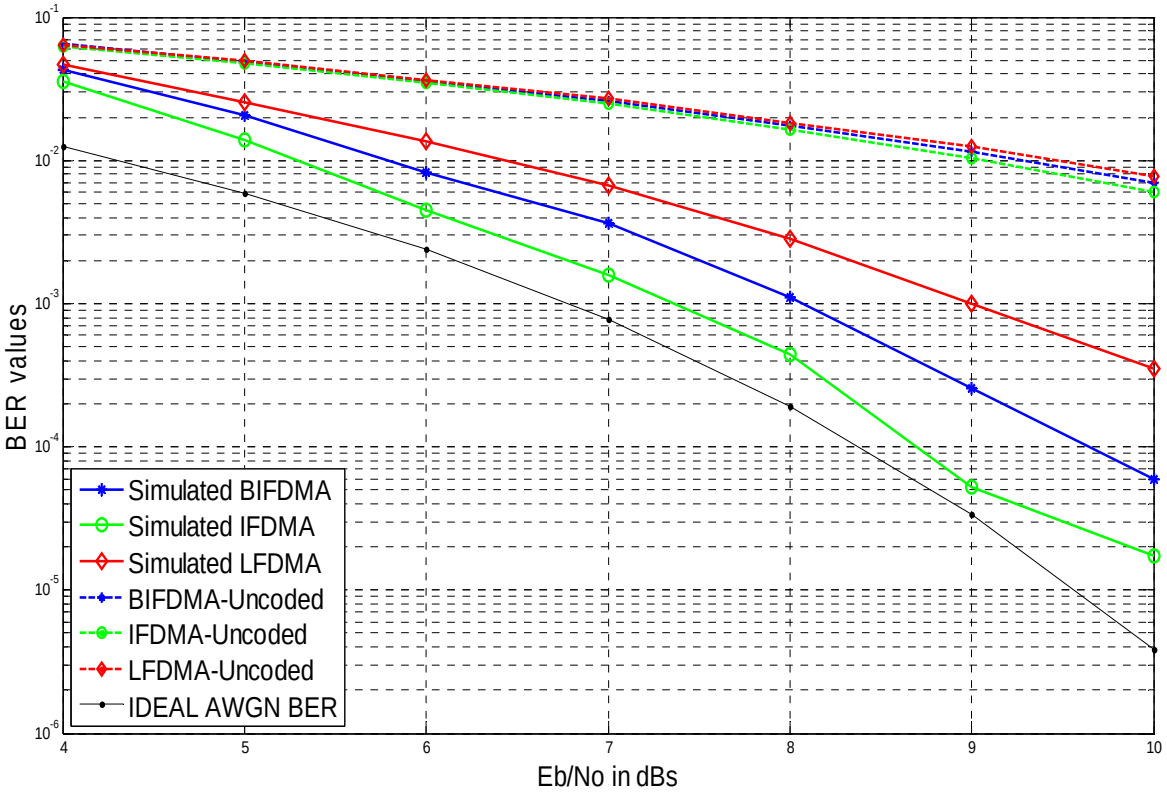

Figure 3.3: Uncoded Vs Turbo Coded Performance on Rayleigh Fading Channel

The figure 3.3 represents the BER performance of the three sub-carrier mapping schemes with and without the Turbo code. The performance of the three schemes in uncoded case is almost similar and much worse than the coded performance. In the Turbo coded case the BER performance of IFDMA is better in comparison to the other two schemes. This is due to the fact that IFDMA collects more frequency diversity compared to BIFDMA which in turn collects more frequency diversity than the LFDMA scheme. This is visible in the figure above as BER performance of IFDMA is followed by BIFDMA and then LFDMA.

3.4.2 MULTI USERS (2, 4, 8)

Case 1: 2 Users:

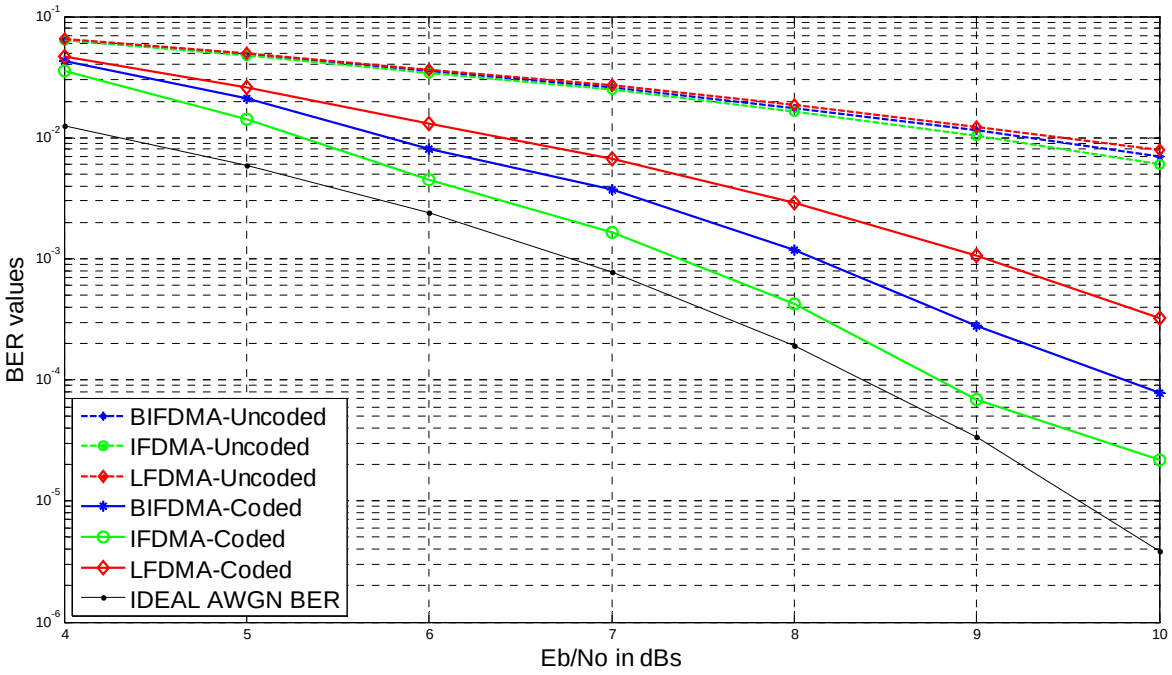

Figure 3.4: Uncoded Vs Turbo Coded Performance for 2-Users

Case 2: 4 Users:

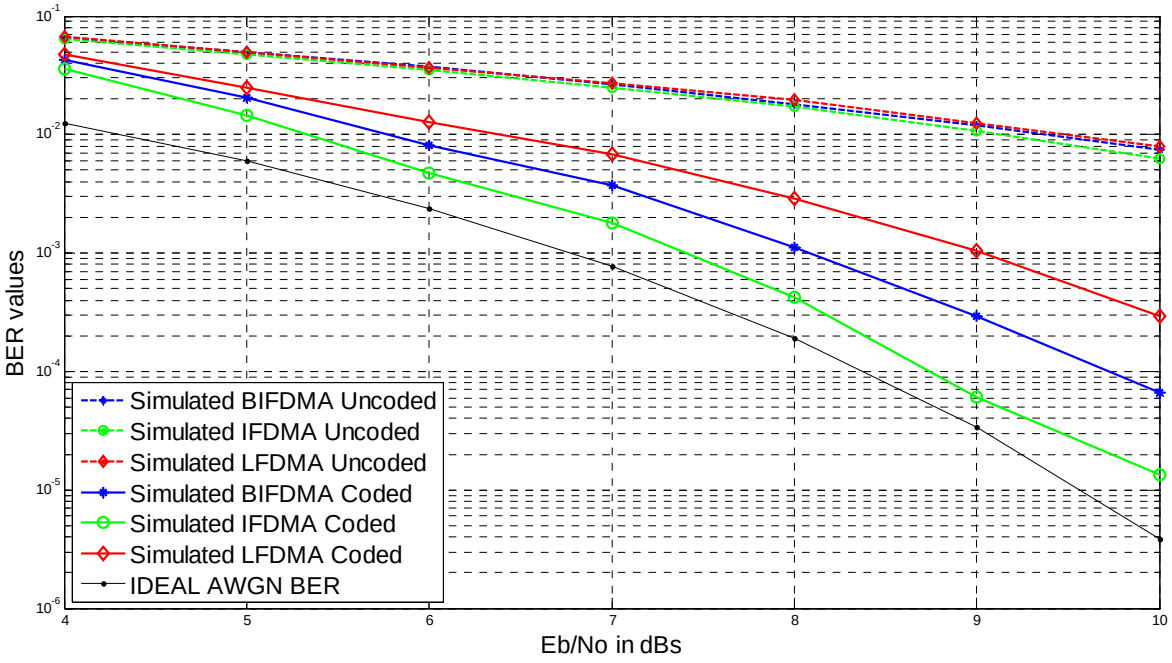

Figure 3.5: Uncoded Vs Turbo Coded Performance for 4-User

Case 3: 8 Users:

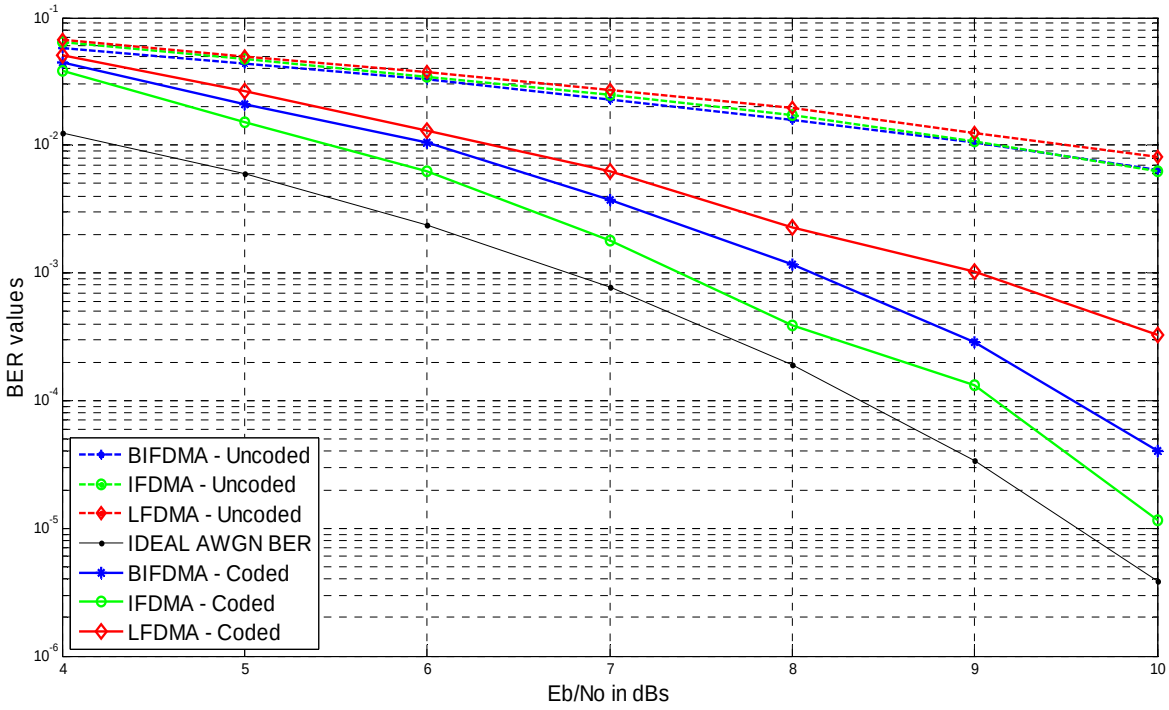

Figure 3.6: Uncoded Vs Turbo Coded Performance for 8-Users

In Multi User Linear Environment as we increase the number of users from two to eight, the long term average BER performance resembles the single user BER performance as shown in figures 3.4, 3.5 and 3.6 above. This is because we do not have any interference in a linear environment. In a non-linear environment the deviation in performance, as we increase the number of users, is more visible due to effect of ICI and MAI. This will be discussed in some more detail later on in the report.

3.5 Performance evaluation of DFT Precoding

In this section we analyze the performance of DFT precoded system compared to a Non DFT precoded system having a single user and multi users in linear environments.

3.5.1 SINGLE USER

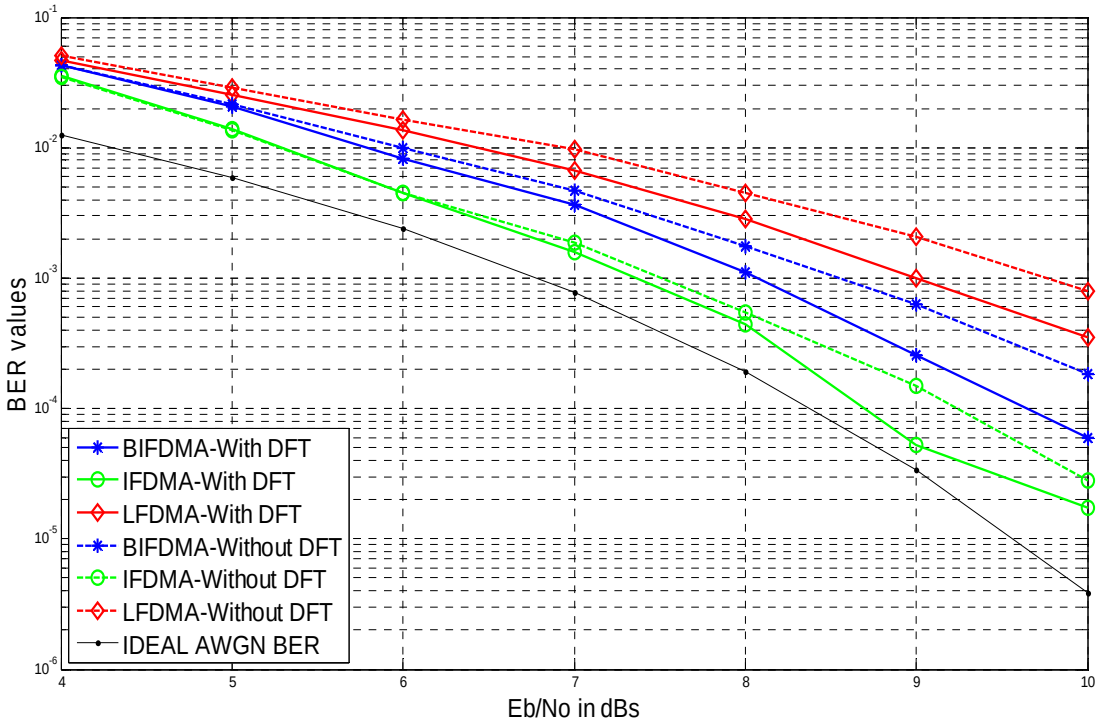

Figure 3.7: DFT precoded Vs Non DFT precoded performance for Single User

The figures 3.7-3.10 show the BER performance analysis of the three subcarrier mapping schemes for a single user and multiple users with respect to DFT precoded and Non DFT precoded system. In all the cases the BER for DFT precoded system is better than the system without DFT precoding. The change in BER beyond approximately 7dBs with DFT precoding compared with Non DFT precoding System is almost same for all the three mapping schemes. The reason behind the lower BER for DFT precoded system is the spreading of each data symbol over multiple sub-carriers that also causes the spreading gain or frequency diversity gain in a frequency selective channel [12]. The difference in BER due to DFT precoding is more visible at higher SNRs.

3.5.2 MULTI USERS (2, 4, 8)

Case 1: 2 Users:

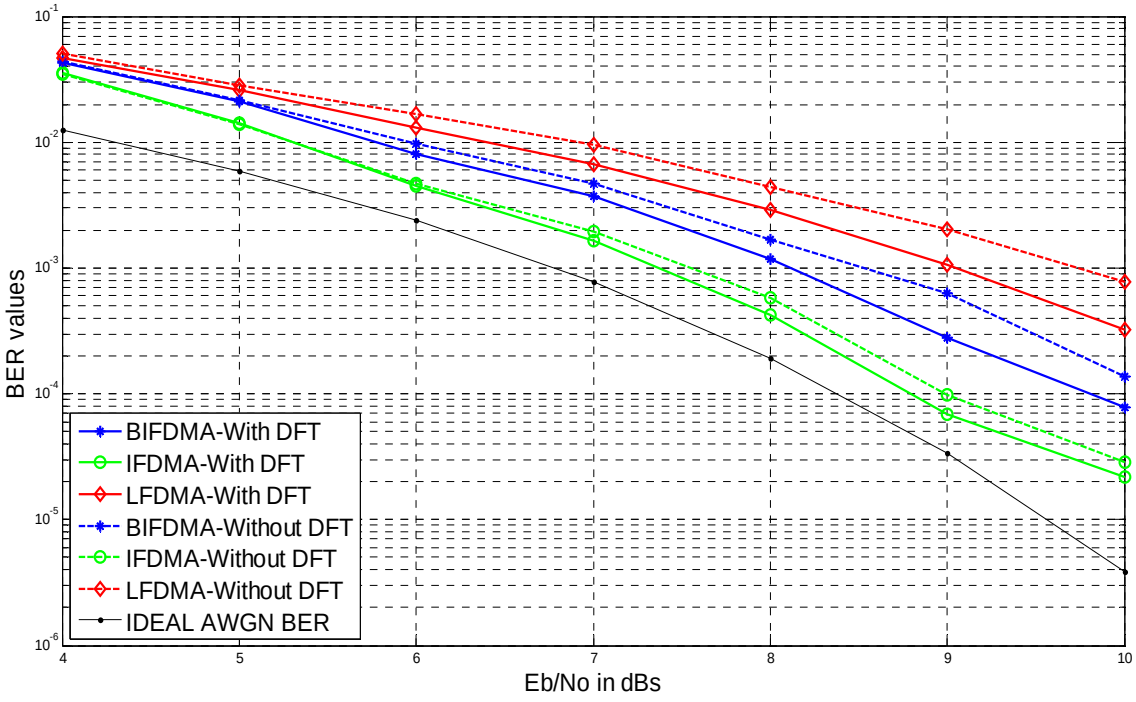

Figure 3.8: DFT precoded Vs Non DFT precoded performance for 2-Users

Case 2: 4 Users:

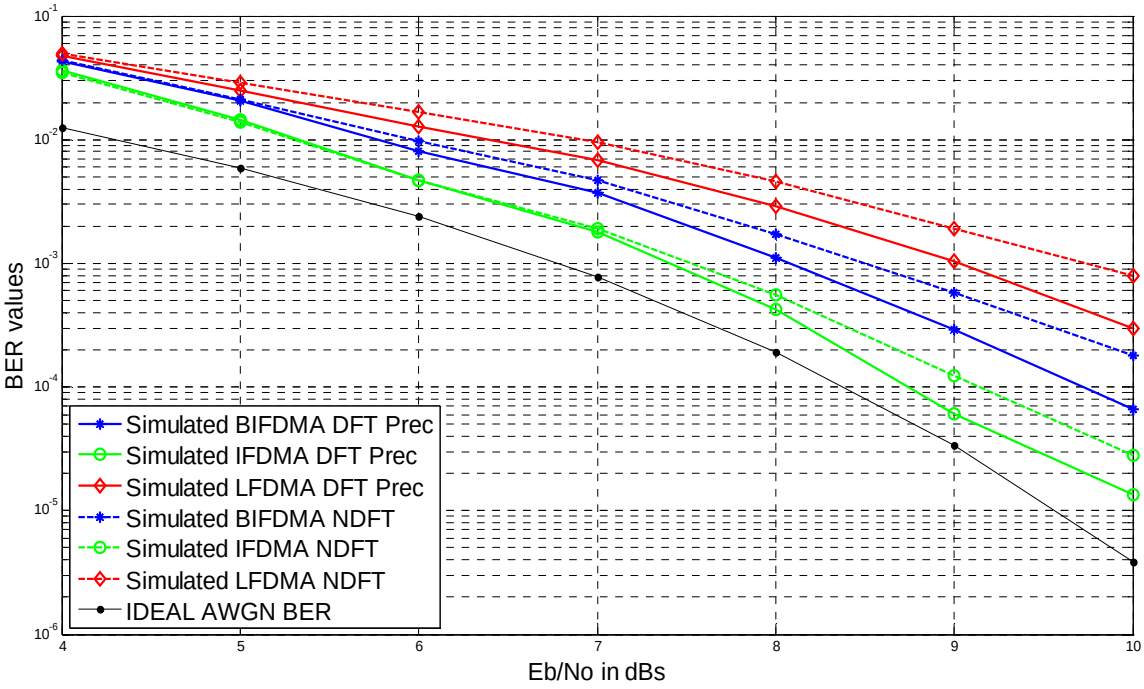

Figure 3.9: DFT precoded Vs Non DFT precoded performance for 4-Users

Case 3: 8 Users:

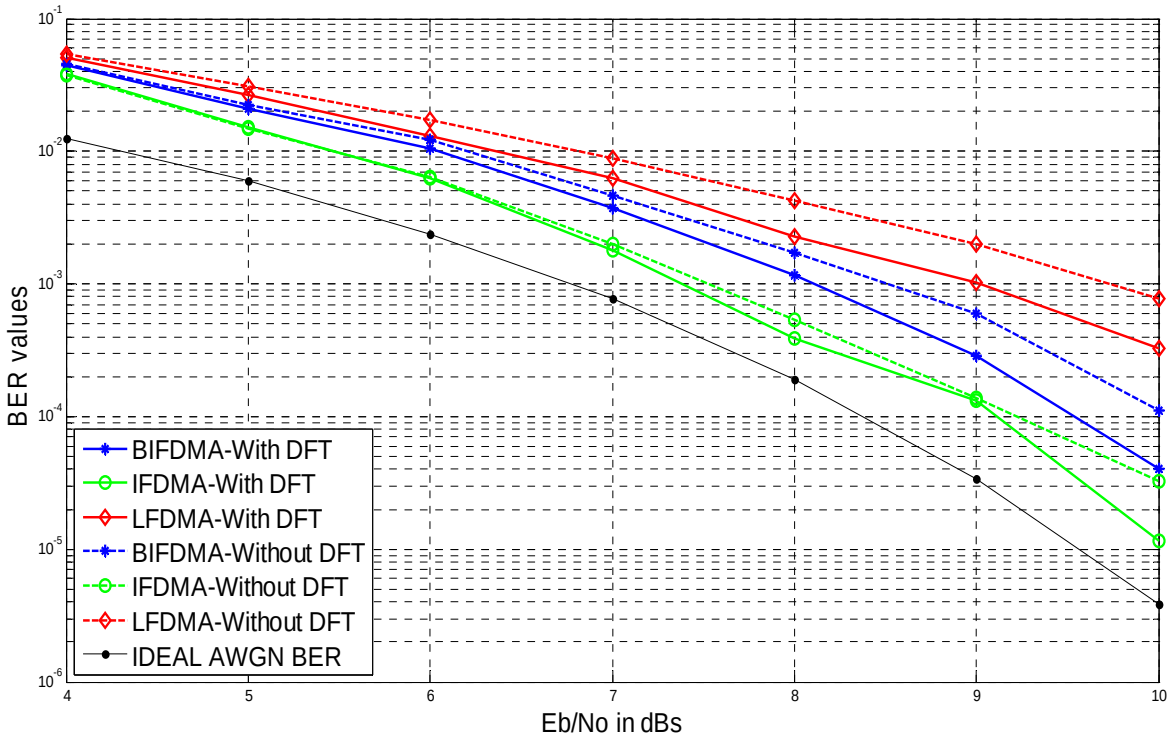

Figure 3.10: DFT precoded Vs Non DFT precoded performance for 8-Users

It is thus clear from the figures above that as was the case in performance evaluation of Turbo coding, here as well, the BER performance for single user is the same as the long term average BER performance for multiuser system. Again this can be motivated by the lack of non-linearities in the system which makes sure that there is no out of band interference in the system. The Performance impact of DFT precoding in non-linear environment will be discussed later on in the report.

3.6 Modeling Amplifier Non-Linearities

The results up to now (except figures 3.1 and 3.2) have been achieved in linear environments where the power in each sub-carrier and each user, in case of multiple users, is limited to itself and does not leak into other sub-carriers and users respectively. Beyond this point, non-linearities are introduced in the system. This is done by employing a threshold clipping device which would clip the signal above certain predetermined threshold. Results include clipping levels of 10% and 30%. It should be noted that clipping the signal will reduce the average energy of the clipped signal which would also result in some difference in BER performance due to the reduction in energy of clipped signal but this is not an interesting result. So we prevent this by rescaling the clipped signal to keep the average energy of the clipped signal the same as the average energy of the input signal to the clipping device. This would enable us to see the effect of only the interference in the BER curves.

3.6.1 INTER CARRIER INTERFERENCE (ICI)

This section of the report deals with a single user simulation done in linear environment and in non-linear environment with different percentage clipping levels to see the effect of ICI.

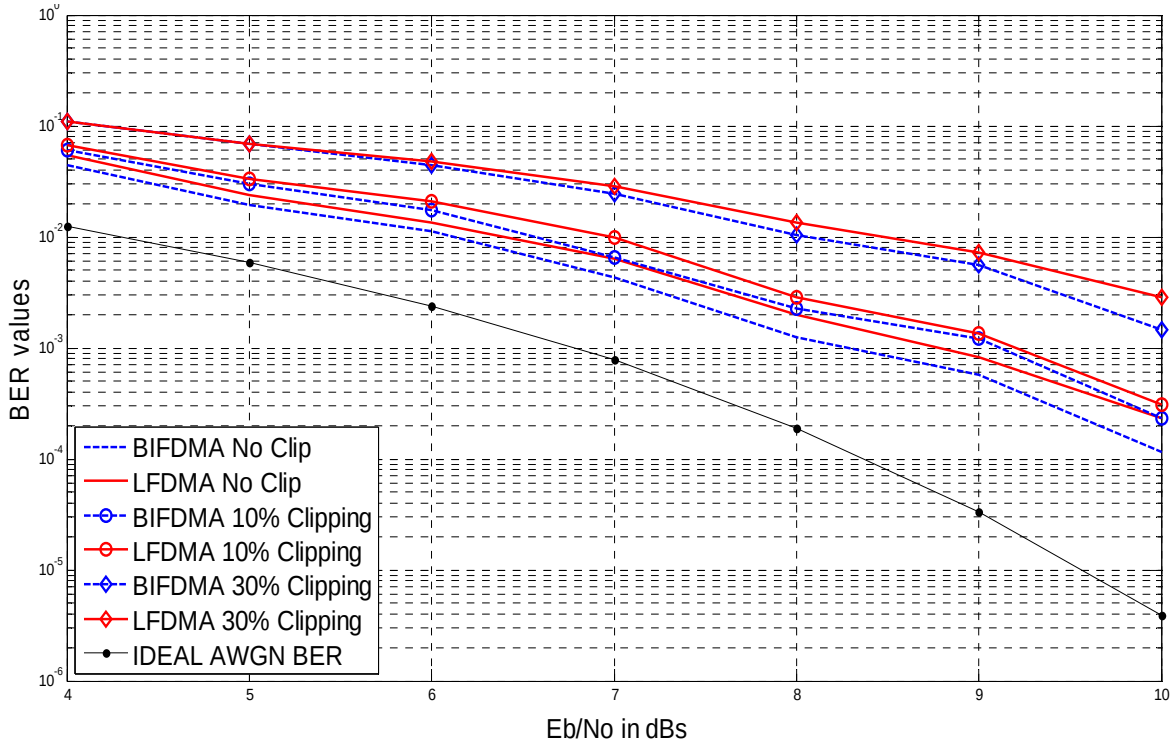

Figure 3.11: Inter Carrier Interference (10%, 30 % and no Clipping)

The figure 3.11 indicates that as the percentage clipping level is increased, the BER performance becomes worse. This is expected as increasing the clipping level will cause increased non-linearities and hence increased power leakage between adjacent sub-carriers i.e. ICI. Rescaling ensures that the variation in BER with increased non-linearities is only due to ICI and not due to any power variation of clipped signal with respect to the unclipped signal. It is noteworthy here that 10% clipping means clipping about 102 samples and 30% clipping means clipping about 307 samples of the total 1024 samples of SC-FDMA symbol.

Moreover the figure above also shows that the BIFDMA performs better than the LFDMA whether we have 10% or 30% clipping. This can be explained as the out of band radiation, caused due to non-linear distortions produced by non-linear amplifier, is dependent on the envelope of the input signal to the amplifier [15]. The envelope fluctuations of BIFDMA in turn are considerably lower than those of LFDMA when we have no over-sampling and no windowing of the signal [10]. Thus these lower envelope fluctuations for BIFDMA may account for the relatively better BER performance of BIFDMA compared to LFDMA in non-linear environments.

3.6.2 PERFORMANCE OF DFT AND NON DFT IN NON-LINEAR ENVIRONMENT

The Performance of DFT precoded system is still better even in non-linear environment as compared to the Non DFT precoded system. In this section we analyze the performance of BIFDMA and LFDMA by introducing non-linearities using two different clipping levels (10% & 30%). The figure 3.12 shows the change in BER of BIFDMA and LFDMA at 10 % and 30 % clipping in presence of DFT and Non DFT precoding. The BER of the Non DFT precoded system is higher than that of DFT precoded system due to the fact that the absence of DFT precoding results in higher envelope fluctuations that would ultimately cause higher out of band interference. Furthermore the BER for BIFDMA is lower as compared to LFDMA as it has comparatively lower envelope fluctuations [10]. Another reason for the low BER for DFT precoded system is the spreading of each data symbol over multiple sub-carriers thus giving frequency diversity as mentioned before. The BER for the two schemes is higher for 30 % clipping than for 10 % clipping due to more samples being clipped with 30% clipping.

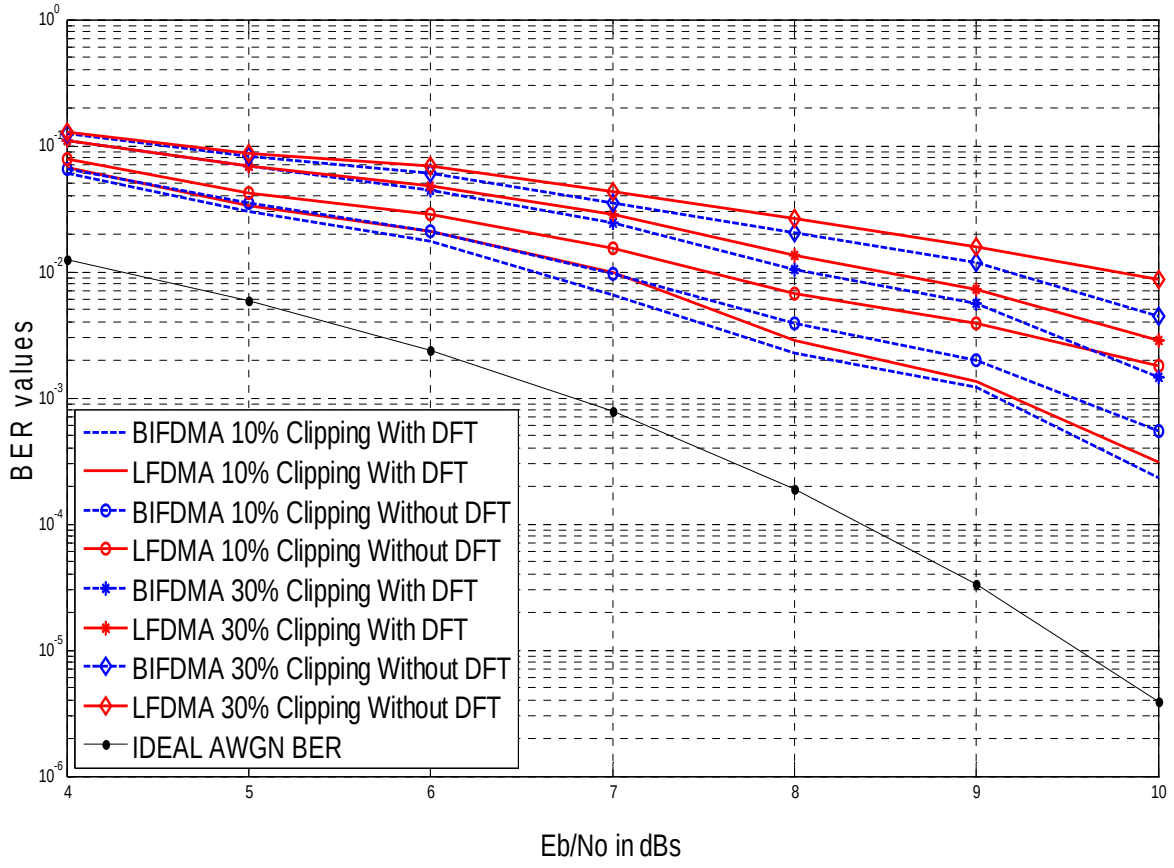

Figure 3.12: DFT & Non DFT precoding System with 10%, 30 % Clipping

3.6.3 MULTI-ACCESS INTERFERENCE (MAI)

In this part of the report we discuss the multi-access interference between multiple users in non-linear environment. Test cases with two, four and eight users have been used and 30% clipping is applied to introduce non-linearities.

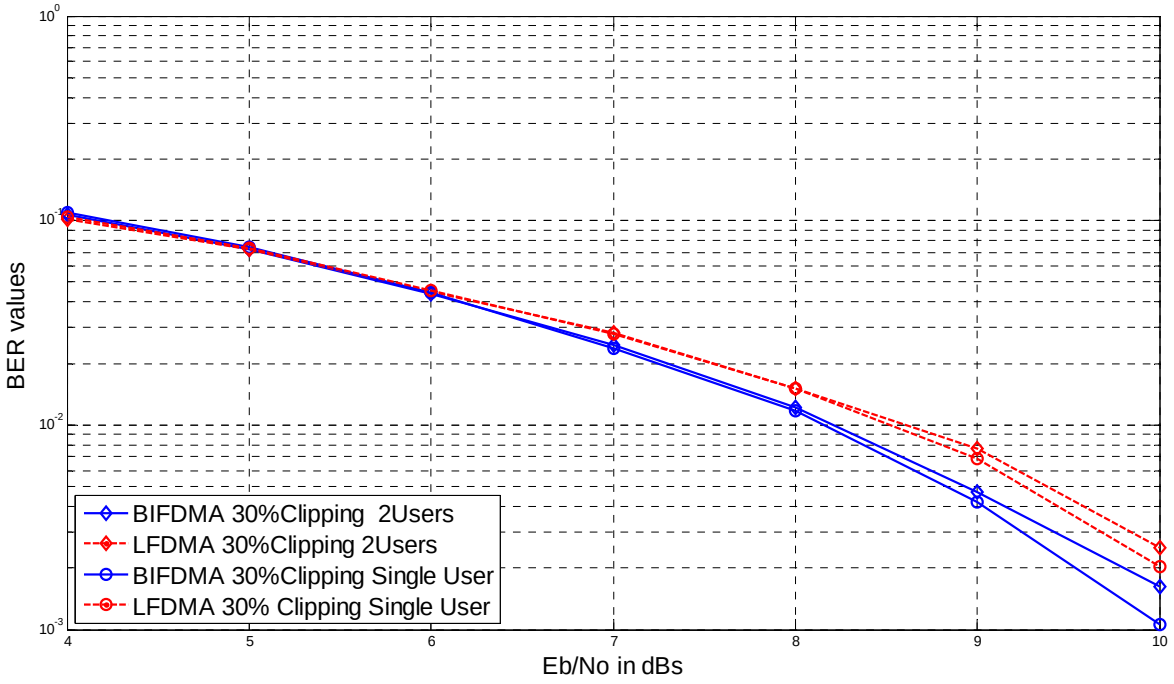

Figure 3.13: Multi-Access Interference with 2-Users

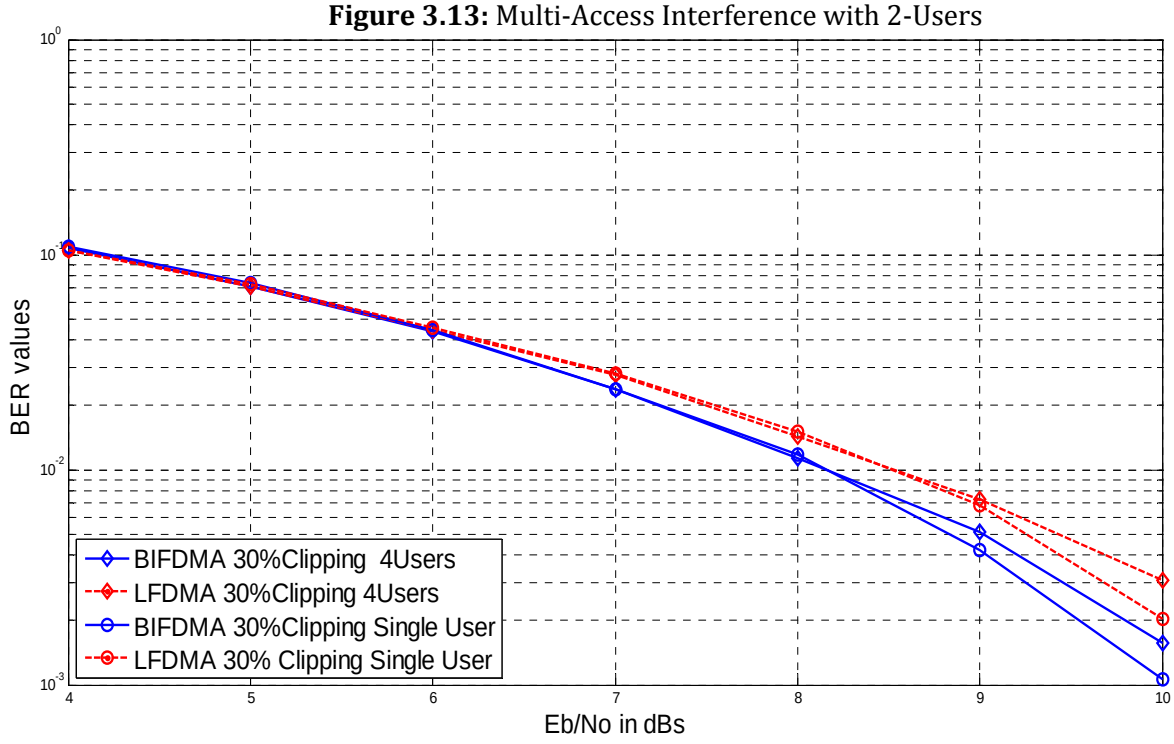

Figure 3.14: Multi-Access Interference with 4-Users

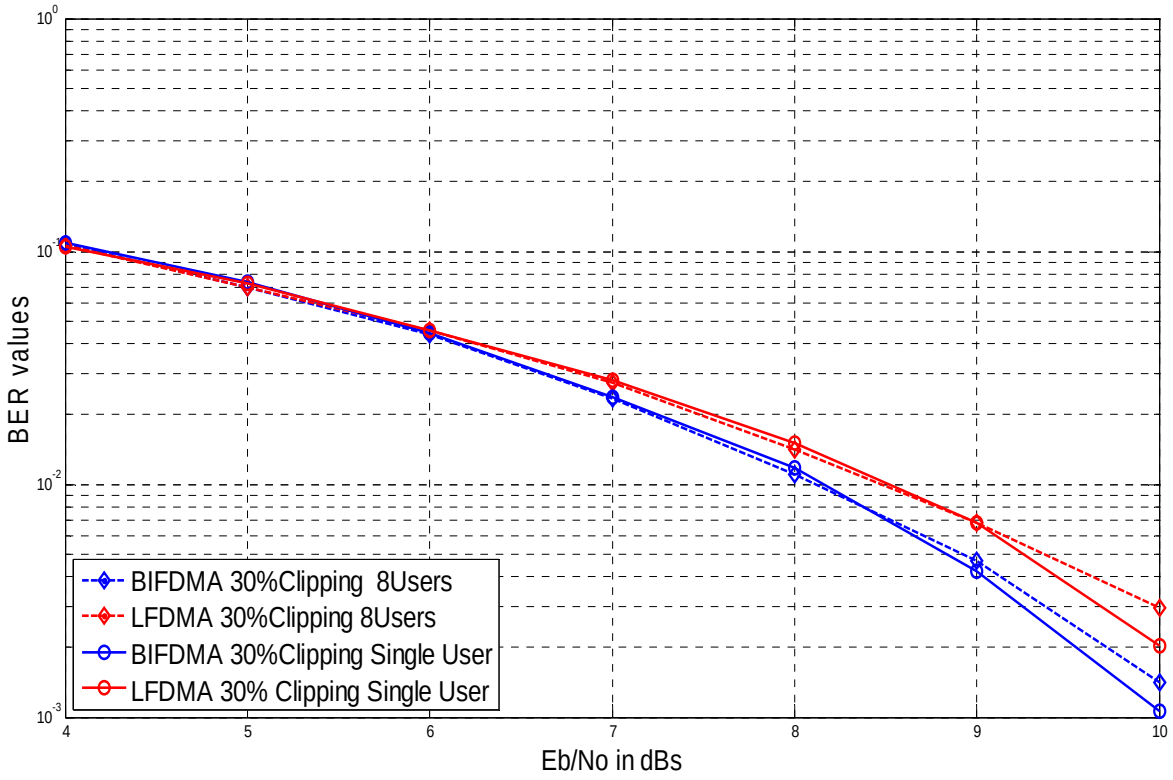

Figure 3.15: Multi-Access Interference with 8-Users

The figures 3.13, 3.14 and 3.15 above clearly indicate that increasing the number of users would worsen the BER performance for both BIFDMA and LFDMA. Again rescaling makes sure that any variation in the long term BER of multiple users relative to BER of single user is purely due to multi-access interference. Increasing the number of users in multiuser non-linear system should increase the multi-access interference which in our case holds true but the variation in BER for different number of users and that for single user is not that evident from the figures above. More over the degradation in BER is more noticeable at higher values of SNRs beyond approximately 8.5dBs. The multi-access interference with 10% clipping for two, four and eight users is depicted in figures in appendix B of this report.

3.7 Multi-Access Interference (MAI) with Near Far Effect

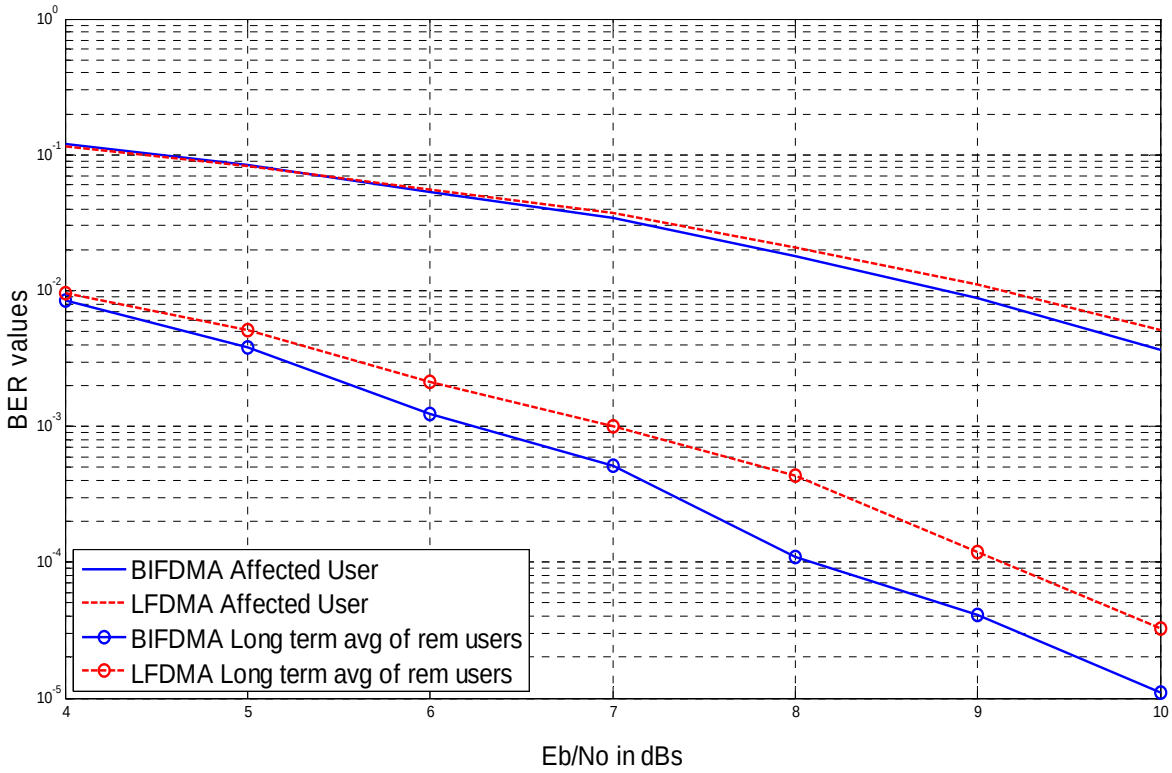

Figure 3.16: Multi-Access Interference with Near Far Effect 8-Users

Near far effect is a phenomenon that is introduced when one mobile user is more near to the base station than the others. In this situation the user that is near to the base station will be receiving higher power than the ones far from it. In figure 3.16, we have analyzed the near far effect in a system having eight users. In this scenario we have one user that is far away from base station while the rest of others are near to it. The affected user (farther from the BS) has been assigned 5dBs less power as compared to the rest of seven users while we have introduced non-linearities in our system by clipping 30% of the samples in the signal. The seven users are rescaled with respect to the affected or weak user so as to eliminate the effect of power change due to clipping while analyzing BER of affected user due to the near far effect.

Chapter 4

Conclusions & Future Work

The chapter includes the summary in terms of our conclusions made from simulations and results. The possible future work related to our thesis is also discussed here.

4.1 Conclusions

In this part of our report, we have described our key findings & conclusions based upon the simulations we did in this thesis.

- The performance of Turbo code over AWGN channel is much better as compared to the fading channel. Moreover owing to the fact that there is no frequency selectivity in AWGN channel both the BIFDMA and LFDMA collects same frequency diversity and hence BER curves for both almost fall over each other. In case of fading channel however BIFDMA performs better than LFDMA owing to its ability to collect more frequency diversity. Non-linearities on the other hand cause slight deviations in the BER curves for the two schemes in both AWGN and fading channel due to out of band interference resulting from non-linearities.
- In linear environments, the BER performance of single user is identical to the long term BER performance of multiple users because of lack of out of band interference as is the case in non-linear environments. IFDMA performs the best in terms of BER which is followed by BIFDMA and then LFDMA. This is because of the ability of IFDMA to achieve more frequency diversity than the other two schemes.
- DFT precoding is mainly intended to keep the PAPR of the signal to a lower level and hence to ensure efficient use of HPA. However DFT precoded system also shows an improvement in BER performance compared to non DFT precoded system owing to the frequency diversity gain in frequency selective channels caused by spreading of each data symbol over multiple sub-carriers.
- BIFDMA and LFDMA perform differently in terms of their BER performances for a single user, in linear environments and in non-linear environments. The reason for this difference in BER performance is the ICI that is caused due to the non-linearities in the system. The ICI increases as the clipping percentage is increased that result in higher non-linearities. This is evident from increased difference in the BER compared to linear case.
- In non-linear environments, DFT precoded systems again have better BER performance compared to non DFT precoded systems. The reason for this is the reduced PAPR caused by DFT precoding which reduces not only envelope

fluctuations but also reduces influence of out of band radiations caused by non-linearities. Similarly BIFDMA also performs better compared to LFDMA in non-linear environments, again due to lower envelope fluctuations in BIFDMA compared to LFDMA.

- In non-linear environments with multiple users, the system suffers from MAI which degrades the BER performance of multiuser system compared to single user system. As the number of users is increased the BER performance worsens due to increased MAI.
- In the multi-user system with non-linearities, the near far effect is evident when few users with high power (near to base station) creates interference for the users that are far away from the base station, resulting in comparatively higher BER for the effected users.

4.2 Future Work

This thesis research work does not include pulse shaping due to which we haven't been able to assess the performance of IFDMA in non-linear environments. In future the simulations can be carried out in presence of pulse shaping to have more realistic comparisons of the three mapping schemes in linear and non-linear environments. Threshold clipping has been used to model the amplifier non-linearities in this thesis work which can be replaced by more sophisticated non-linearity models like the Rapp model. The impact of carrier frequency offset (CFO) and Doppler can also be included to in the future research work. Finally the channel scenario being used in this thesis work is the WINNER-C2 NLOS. It can be an interesting option to use other channel scenarios.

Appendix-A

SIMULATION OF RAYLEIGH FADING CHANNEL

In this Appendix we have described spectrum method by which we have simulated our channel. There are two methods to simulate Rayleigh fading channel, one is "Filter method" and the other one is "Spectrum method". Filter method is more accurate but more complex as compared to the spectrum method, this is due to the convolution process which is replaced by the multiplication in spectrum method.

A.1 Spectrum Method

In the spectrum method, the complex gain of the channel *c(t)* is calculated in the frequency domain that has been shown in the equation below.

$$C(f) = X(f)G(f) \tag{1}$$

Where *C(f)* is the Fourier transform of the channel gain *c(t)*, *G(f)* is the frequency response of the filter while *X(f)* is the Fourier transform of the input to the filter *x(t)*. Where *x(t)* is complex wide Gaussian Noise with unit power spectral density. The samples of *c(t)* that is *c(nTs)* is then computed as inverse Fourier transform of the samples of *C(f)* [6].

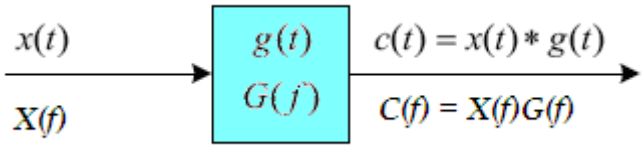

Figure A.1: Channel gain as the output of a linear filter

In spectrum method, *"Ts"* is chosen such that, $fs = 1/Ts > 2f_D$. This makes sure that no aliasing occurs. After that, $\hat{G}(f)$ is formed from *G(f)* as $\hat{G}(f) = G(f) + G(f - fs)$. Then "*Ns*" samples of $\hat{G}(f)$ are formed as $\hat{G}(kfs/Ns)$ where *k* = 0, 1, ... , *Ns-1.* Finally *c(nTs)* is computed as an *Ns*-point inverse FFT of $\hat{G}(kfs/Ns)$ Z (*k*), where *Z(k)* for k= o, 1, ... , *Ns* – 1

are independent, zero mean, complex Gaussian random variables. The variance of *Z(k)* is chosen such that *c(nTs)* will have unit variance [6].

A.2 Time & Frequency Varying Rayleigh Fading Channel

In this section we have explained how to simulate a time frequency varying channel using the complex channel gains obtained from the spectrum method. A discrete-time model of such a channel with "L" taps and sample interval Ts is shown in figure below,

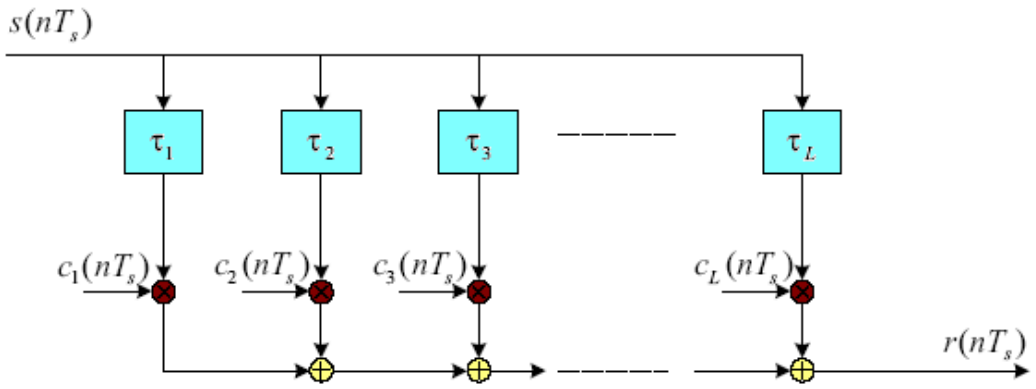

Figure A.2: Discrete-time model of a time and frequency-varying channel

The $C_l(nTs)$ represents the tap gains for each channel tap. The tap gains would amplitude scale any signal passing through any particular channel tap. The time and frequency varying response, *C (f, nTs)* is the amplitude scaling a complex exponential with frequency "*f*" experiences, when it is transmitted over the channel [6]. So we have that

$$C(f, nTs) = \sum_{l=1}^{L} c_l(nTs)\exp(-j2\pi f\tau_l T_s) \qquad (2)$$

Where "τ_l" is the tap delay for each channel tap. For frequencies f = *k*/ (*NTs*) where *k = 0,1, ... , N-1.* The equation 2 can be simplified as

$$C(k/(NTs), nTs) = \sum_{l=1}^{L} c_l(nTs)\exp(-j2\pi\tau_l k/N)$$

$$\stackrel{\Delta}{=} C[k, n] \qquad (3)$$

The time frequency varying response for WINNER-C2 NLOS with 1000 time samples and 128 Frequency samples is shown in the figure below,

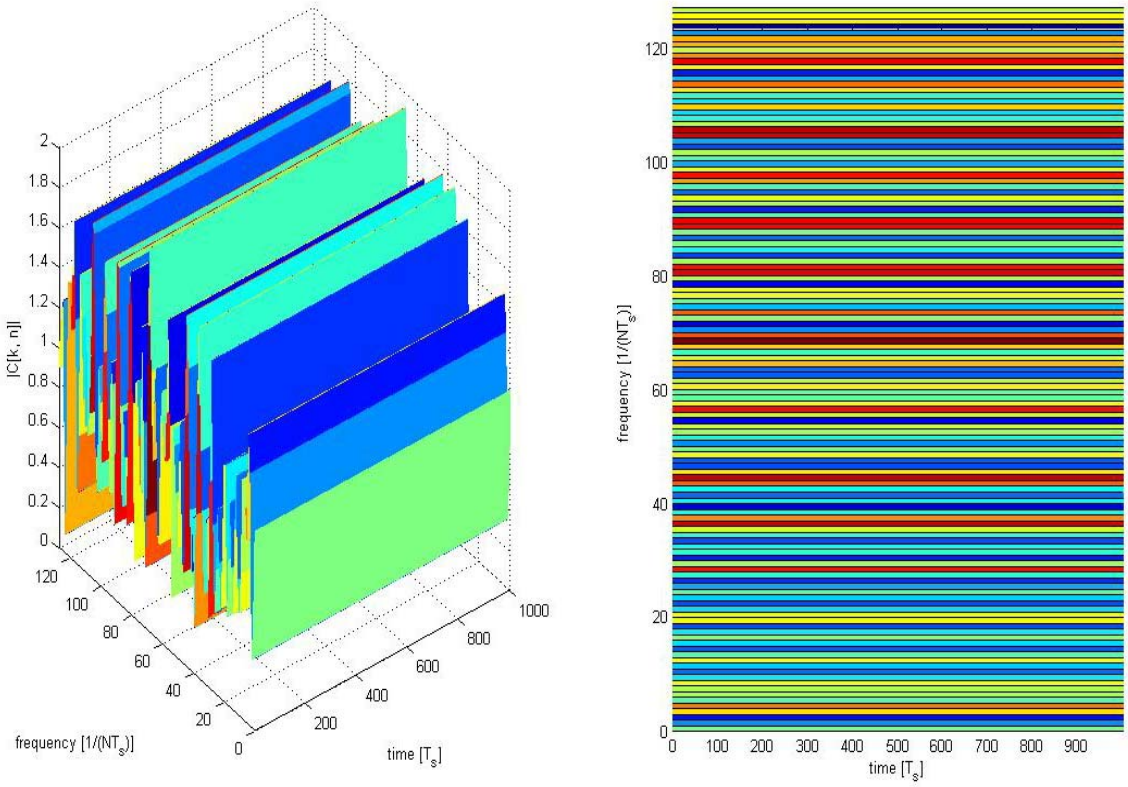

Figure A.3: Time and Frequency Response of WINNER–C2 NLOS Channel

Appendix-B

Additional Results

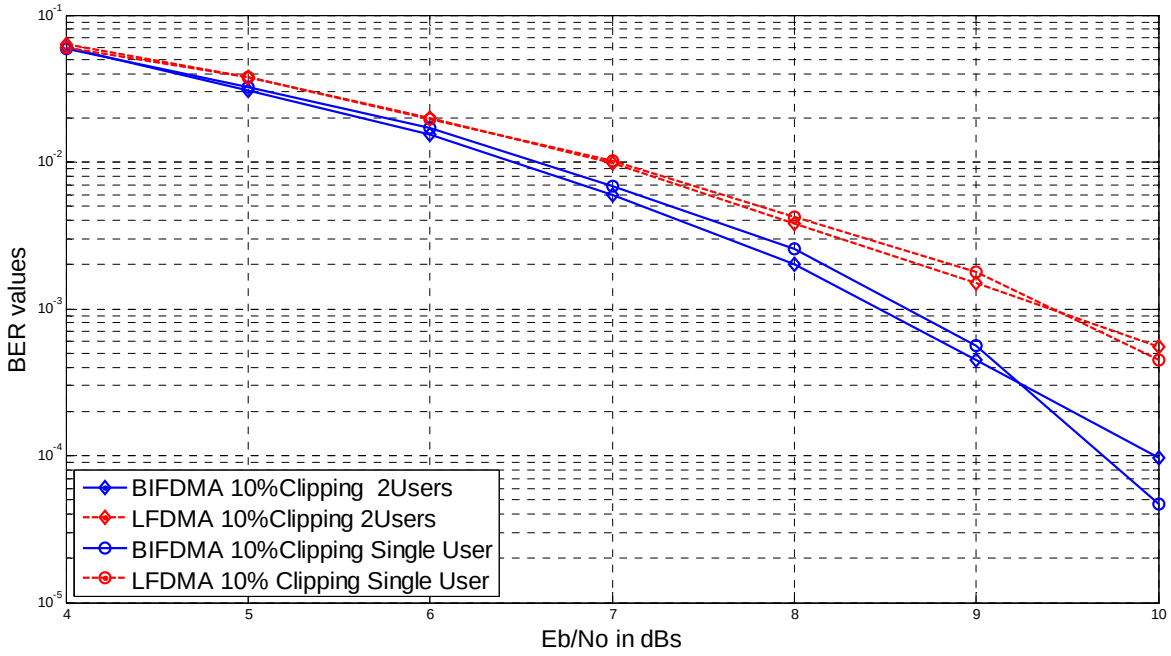

Figure B.1: Multi-Access Interference with 2-Users (10 % Clipping)

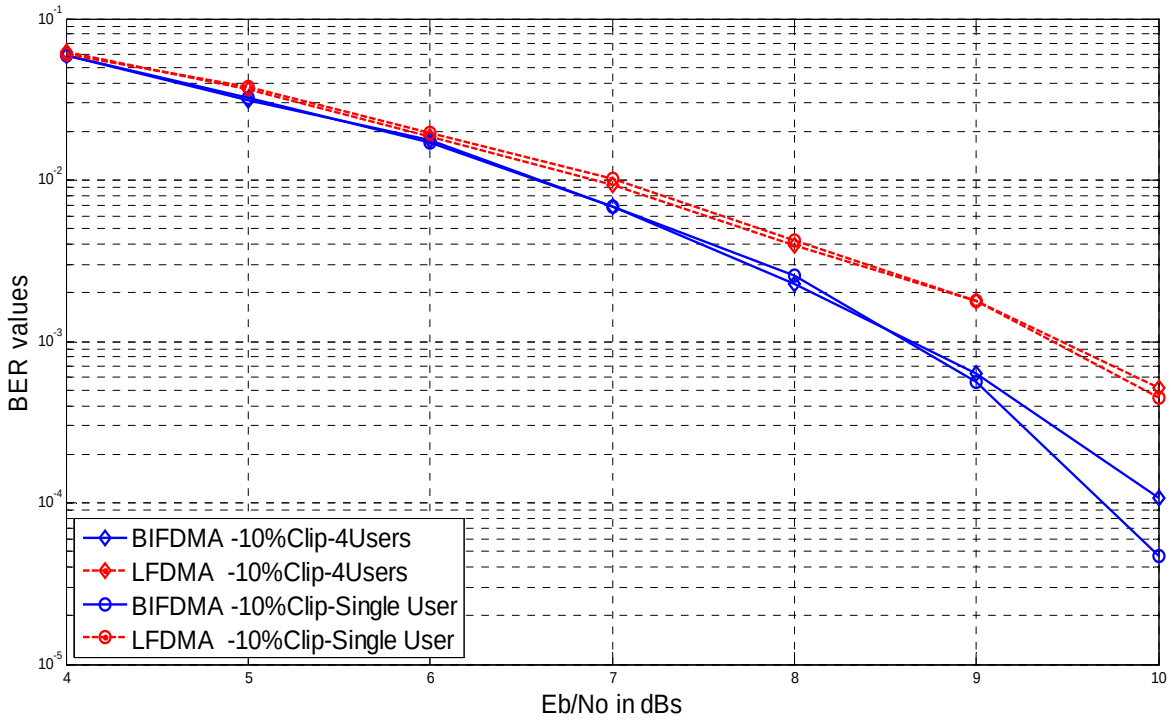

Figure B.2: Multi-Access Interference with 4-Users (10 % Clipping)

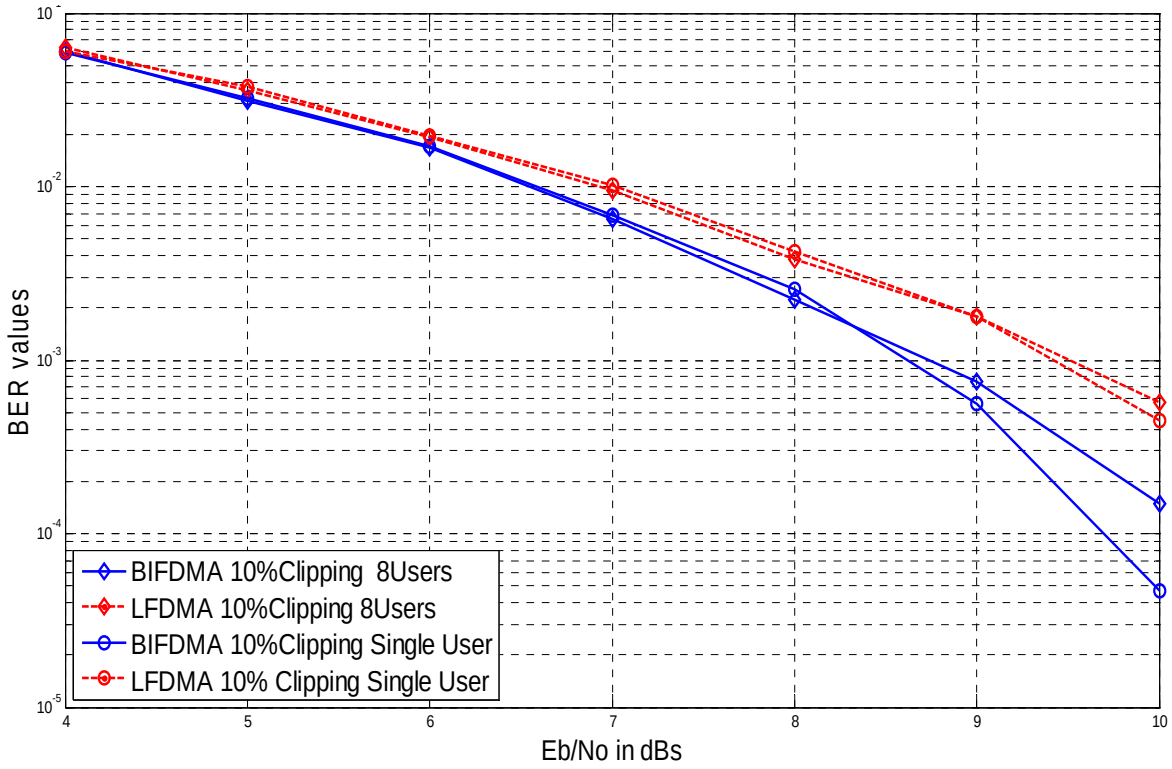

Figure B.3: Multi-Access Interference with 8-Users (10 % Clipping)

References

[1] Goldsmith, Andrea. Wireless Communications. New York: Cambridge University Press; 2005.

[2] Dahlman E, Parkvall S, Sköld J, Beming P. 3G Evolution HSPA and LTE for Mobile Broadband. London: Academic Press Inc; 2007.

[3] Madhow Upamanyu. Fundamentals of Digital Communications. New York: Cambridge University Press; 2008.

[4] Puckett W. Bruce. Implementation and Performance of an Improved Turbo Decoder on a Configurable Computing Machine. Master's Thesis Report. Virginia: Virginia Polytechnic Institute and State University; 2000.

[5] Rehman Mujeeb Ur, Jälmbrant Ulf, Ahmed Ameer. Channel Coding. Group Project report. Project 2. Digital communication Course. Göteborg: Chalmers University; 2008.

[6] Ström Erik, Seifi Nima Simulation of fading wireless channel. Technical report. Project 1. Wireless Communication Course. Göteborg: Chalmers University; 2009.

[7] Ramana D.Venkata, Pal Surendra, Prasad A.P.Shiva. Simulation and realization of Baseband pulse shaping filter for BPSK modulator; 2004.

[8] Hsu Hwei P. Schaum's outline of theory and problems of analog and digital Communications.Montville: McGraw-Hill Companies; 2003.

[9] Srikar Leela M, Karrout Johnny. Uplink Multiple Access For IMT-Advanced. Master's Thesis Report. Göteborg: Chalmers University; 2009.

[10] Frank Tobias, Klein Anja, Haustein Thomas. A Survey on the Envelope Fluctuations of DFT Precoded OFDMA Signals. International Conference on Communications ICC. Beijing; 2008.

[11] Astély David, Dahlman Erik, Furuskär Anders, Jading Ylva, Lindström Magnus, Parkvall Stefan. LTE: The Evolution of Mobile Broadband. IEEE Communications Magazine. Ericsson Research; 2009.

[12] SC-FDMA Single Carrier FDMA in LTE. IXIA Worldwide Headquarters. Calabasas, CA; 2009.

[13] Scheim Jacob. SC-FDMA for 3GPP-LTE. Communication and Signal Processing Limited; 2008.

[14] Svensson T, Frank T, Falconer D, Sternad M, Costa E, Klein A. B-IFDMA - A Power Efficient Multiple Access Scheme for Non-Frequency-Adaptive Transmission. Mobile & Wireless Communications Summit. Budapest; 2007.

[15] Svensson T, Frank T, Eriksson T, Aronsson D, Sternad M, Klien A. Block Interleaved Frequency Division Multiple Access for Power Efficiency, Robustness, Flexibility, and Scalability. EURASIP journal on Wireless Communications and Networking. Hindawi Publishing Corporation; 2009.

[16] Myung Hyung G. Single carrier FDMA. Presentation Slides; 2008. (hgmyung.googlepages.com/scfdma.pdf)

[17] Mach Pavel, Bešťák Robert. Implementation of OFDM into Broadband Wireless Networks. Department of Telecommunication Engineering. Prague: Czech Technical University in Prague.

[18] Sari Hikmat. OFDM Peak Power Reduction Techniques Performance Analysis for WiMAX Systems. Presentation Slides. 4th Annual Wireless Broadband Forum. Cambridge; 2005.

[19] Rapp Christoph. Effects of HPA-non-linearity on a 4-DPSK/OFDM signal for a digital sound broadcasting system. 2nd European Conference on Satellite Communications. Liege; 1991.

[20] Chaniotakis M, Cory D. Transistors: Bipolar Junction Transistors (BJT); 2006.

[21] Ma Xiaoqiang, Kobayashi H, Schwartz Stuart C, Zhang J, Gu Daqing. Iterative Channel estimation for OFDM with Clipping. 5th International Symposium on Wireless Personal Multimedia Communications. Hawaii; 2002.

[22] Svensson Tommy. UL Power Control, Efficiency and Performance Assessment Criteria. CELTIC Wireless World Initiative New Radio+ (WINNER+) Seminar. Göteborg; 2007.

[23] R4-060867. Uplink Power Control for E-UTRA. Tallinn; 2006.

[24] Muhammad Bilal. Closed loop power control for LTE uplink. Master's Thesis Report. Karlskrona: Blekinge Tekniska Hogskola; 2008.

[25] Skillermark Per. Uplink Power Control. CELTIC Wireless World Initiative New Radio+.

[26] Quintero Nestor J. Advanced Power Control for UTRAN LTE Uplink. Master's Thesis Report. Aalborg: Aalborg University; 2008.